https://ntrs.nasa.gov/search.jsp?R=19800016716 2020-03-21T18:36:21+00:00Z

N O T I C E

THIS DOCUMENT HAS BEEN REPRODUCED FROM MICROFICHE. ALTHOUGH IT IS RECOGNIZED THAT CERTAIN PORTIONS ARE ILLEGIBLE, IT IS BEING RELEASED IN THE INTEREST OF MAKING AVAILABLE AS MUCH INFORMATION AS POSSIBLE

DOE/NASA/0008-79/10
NASA CR-159713

(NASA-CR-159713) FEASIBILITY STUDY OF SILICON NITRIDE REGENERATORS (Ford Motor Co.) 58 p HC A04/MF A01 CSCL 13F

N80-25209

Unclas
G3/85 20960

FEASIBILITY STUDY OF SILICON NITRIDE REGENERATORS

C. A. Fucinari and V. D. N. RAO
Research Staff
Ford Motor Co.

October 1979

Prepared for
NATIONAL AERONAUTICS AND SPACE ADMINISTRATION
Lewis Research Center
Under Contract DEN 3-8

JUN 1980
RECEIVED
NASA STI FACILITY
ACCESS DEPT.

For
U.S. DEPARTMENT OF ENERGY
Automotive Technology Division

NOTICE

This report was prepared to document work sponsored by the United States Government. Neither the United States nor its agent, the United States Energy Research and Development Administration (now Department of Energy), nor any Federal employees, nor any of their contractors, subcontractors or their employees, makes any warranty, express or implied, or assumes any legal liability or responsibility for the accuracy, completeness, or usefulness of any information, apparatus, product or process disclosed, or represents that its use would not infringe privately owned rights.

DOE/NASA/0008-79/10
NASA CR-159713

FEASIBILITY STUDY OF SILICON NITRIDE REGENERATORS

C. A. Fucinari and V. D. N. Rao
Research Staff
Ford Motor Co.

October 1979

Prepared for
National Aeronautics and Space Administration
Lewis Research Center
Cleveland, Ohio 44135
Under Contract DEN 3-8

For
U.S. DEPARTMENT OF ENERGY
Automotive Technology Division

TABLE OF CONTENTS

Page No.

List of Illustrations ii
List of Tables iv
Summary 1
Introduction 3
Discussion of Results 3

1.0 Background 3
1.1 Engine History 3
1.2 Exhaust Gas Environment in the Gas Turbine Engine 5
1.3 Status of Oxide Ceramic Materials 8

2.0 Silicon Nitride Material Properties 13
2.1 Introduction 13
2.2 Thermal Stability 13
2.3 Oxidation Resistance 14
2.4 Resistance to Chemical Attack 14

3.0 Manufacturing Processes 18
3.1 Reaction Bonded Silicon Nitride 18
3.2 Cost Considerations 18

4.0 Thermal Stress 21

5.0 Aerothermodynamic Performance 39
5.1 Performance Parameters 39
5.2 Influence of Silicon Nitride on Regenerator Package Size 41

References 50
Appendix 51

LIST OF ILLUSTRATIONS

		Page No.
Figure 1.1.1	Core Failure Caused by Chemical Attack.	4
Figure 1.2.1	Regenerator Inlet Temperatures Vs. Gas Generator Speed	7
Figure 1.3.1	Supplier A, AS; Thermal Stability With and Without Sodium at 800°C to 1200°C.	9
Figure 1.3.2	Supplier K, MAS Glass Frit; Thermal Stability With and Without Sodium at 800°C to 1200°C.	11
Figure 1.3.3	Supplier G, MAS Mineral Base; Thermal Stability With and Without Sodium at 800°C to 1200°C.	12
Figure 4.1	Tangential Thermal Stress Distribution at Regenerator Hot Face.	21
Figure 4.2	Thermal Expansion Characteristics of Various Materials.	22
Figure 4.3	Maximum Tangential Stress Ratio Vs. Regenerator Outer to Seal Inner Radius Ratio.	24
Figure 4.4	Maximum Tangential Stress Ratio Vs. Elastic Modulus Ratio.	24
Figure 4.5	Three Dimensional Finite Element Model	25
Figure 4.6	Axisymmetric Stress Analysis Model	26
Figure 4.7	Membrane Element Stress Analysis Model	27
Figure 4.8	Tangential Thermal Stress for 2.7gm/cc Density Silicon Nitride at 1093°C (2000°F)	30
Figure 4.9	Tangential Thermal Stress for 2.3gm/cc Density Silicon Nitride at 1093°C (2000°F)	31
Figure 4.10	Tangential Thermal Stress for 2.7gm/cc Density Silicon Nitride at 1204°C (2200°F)	32
Figure 4.11	Tangential Thermal Stress for 2.3gm/cc Density Silicon Nitride at 1204°C (2200°F)	33

LIST OF ILLUSTRATIONS

Page No.

Figure 4.12 Radial Thermal Stress for 2.7gm/cc Density Silicon Nitride at 1093°C (2000°F) 34

Figure 4.13 Radial Thermal Stress for 2.3gm/cc Density Silicon Nitride at 1093°C (2000°F) 35

Figure 4.14 Radial Thermal Stress for 2.7gm/cc Density Silicon Nitride at 1204°C (2200°F) 36

Figure 4.15 Radial Thermal Stress for 2.3gm/cc Density Silicon Nitride at 1204°C (2200°F) 37

Figure 5.1.1 Regenerator Performance with Respect to Package Size and Fin Parameters for Constant Flow Conditions 44

Figure 5.1.2 Regenerator Performance Zones 45

Figure 5.1.3 Thermal Conductivity with Respect to Package Size and Fin Parameters for Constant Flow Conditions 46

LIST OF TABLES

Page No.

Table 4.1 Silicon Nitride Material Properties 28

Table 4.2 Silicon Nitride Regenerator Thermal Stress 38

Table 5.2.1 Regenerator Flow Conditions 47

Table 5.2.2 Regenerator Matrix Fin Parameters 48

Table 5.2.3 Regenerator Aerothermodynamic Performance 49

SUMMARY

This report examines the feasibility of silicon nitride as a regenerator matrix material for regenerator applications requiring inlet temperatures above 1000°C (1832°F). Using the present generation oxide ceramics (A-S and MAS) as a reference, silicon nitride was examined from a material characteristics, manufacturing, thermal stress and aerothermodynamic performance viewpoint. The results are summarized as follows:

Material Properties — In the regenerator application the matrix temperature can vary from 100°C to 1200°C. The enormous amount of reaction surface due to the high surface to volume ratio of the matrix geometry presents a likely situation for the condensation and accumulation of salts. On the basis of the evidence presented, silicon nitride is adequate at these temperatures provided a surface treatment can be developed to provide sufficient oxidation resistance at 1100°C and below where the sodium salts are in a condensed (liquid) state. For clean sodium free fuel applications the silicon nitride matrices can be expected to perform adequately at temperatures up to 1350°C.

Manufacturing Processes — On the basis of raw material, fabrication, firing and machining costs it appears that the silicon nitride regenerators can be readily mass produced at a cost competitive with those of the oxide base ceramic materials. The cost of the additional surface treatment required for oxidation resistance will determine the ultimate cost effectiveness of a silicon nitride regenerator.

Thermal Stress — The feasibility of silicon nitride with respect to thermal stress capacity appears to be promising. Depending on the thermal stress factor (θ) for the candidate matrix materials, stress relief techniques may or may not be required.

Aerothermodynamic Performance — A substantial increase in heat exchanger volume would be required to attain equivalent performance with that of an oxide base ceramic regenerator due to the much higher thermal conductivity of the silicon nitride material. In order to minimize conduction losses it would be desirable to package the silicon nitride regenerator with a higher length to frontal area ratio by incorporating less compact fin geometries. This factor can create additional complexities to engine packaging requirements.

INTRODUCTION

The efficiency of a gas turbine engine is directly related to the temperature difference between the inlet air to the compressor and exhaust gas from the turbine. Future high temperature passenger car gas turbine engines, to be competitive, may expose the regenerator to inlet temperatures as high as 1200°C (2192°F).

One of the tasks of the current NASA/Ford "Ceramic Regenerator Systems Development Program" is to determine the upper temperature limit for the present generation of oxide ceramic regenerator materials. In the event these materials are not suitable for 1200°C (2192°F) application, existing materials with higher temperature capability such as silicon nitride must be considered.

This report will examine the feasibility of silicon nitride as a viable regenerator material for 1200°C (2192°F) gas turbine engine application. Based on limited available solid and matrix sample material data, silicon nitride will be examined from a thermal stress, oxidation resistance, manufacturing feasibility, and regenerator performance viewpoint. Its advantages and limitations as a regenerator core will be discussed in detail. The report will not take into account the impact of silicon-nitride on the regenerator seal or drive system.

DISCUSSION OF RESULTS

1.0 BACKGROUND

1.1 ENGINE HISTORY

Since 1965, Ford Motor Company has been engaged in developing a ceramic rotary heat exchanger system for use in gas turbine engines, Stirling engines, and waste heat recovery devices. To date over 300,000 hours of engine operating experience have been accumulated on a sample of approximately 1250 regenerator cores fabricated from different materials by a variety of different suppliers utilizing several different manufacturing processes.

Since 1974, this development program has been supported by EPA, ERDA, and at the present time NASA on a cost-sharing basis. The current "Ceramic Regenerator Systems Development Program" has been primarily concerned with demonstrating the successful application of oxide ceramic regenerators in the Ford 707 industrial gas turbine engine at inlet temperatures of 800°C (1472°F) and 1000°C (1832°F).

The development effort at Ford Motor Company has focused on three ceramic matrix materials for the regenerator application. Prior to 1974, over 100,000 hours of engine operating experience were accumulated on a sample of approximately 1000 regenerator cores fabricated from lithium aluminum silicate (LAS) culminating in the determination that this material is not suitable for regenerator service due to a propensity for failure as a result of chemical attack from sodium or sulfur encountered in common road salt and diesel fuel respectively.

 PRECEDING PAGE BLANK NOT FILMED

Sodium, which enters the engine through ingestion of road salt or salt water or from contaminated fuel, attacks the hot side of the regenerator and causes deterioration of material properties. Sulphuric acid, which is formed in the products of combustion, condenses out in the cold side of the regenerator and causes a deterioration of material properties on this face. This sodium and sulphuric acid attack progresses to the point where cracks are formed due to a change in thermal expansion and material growth. Figure 1.1.1 shows typical chemical attack cracks which have propagated radially inward, connected together, and caused the hub to separate.

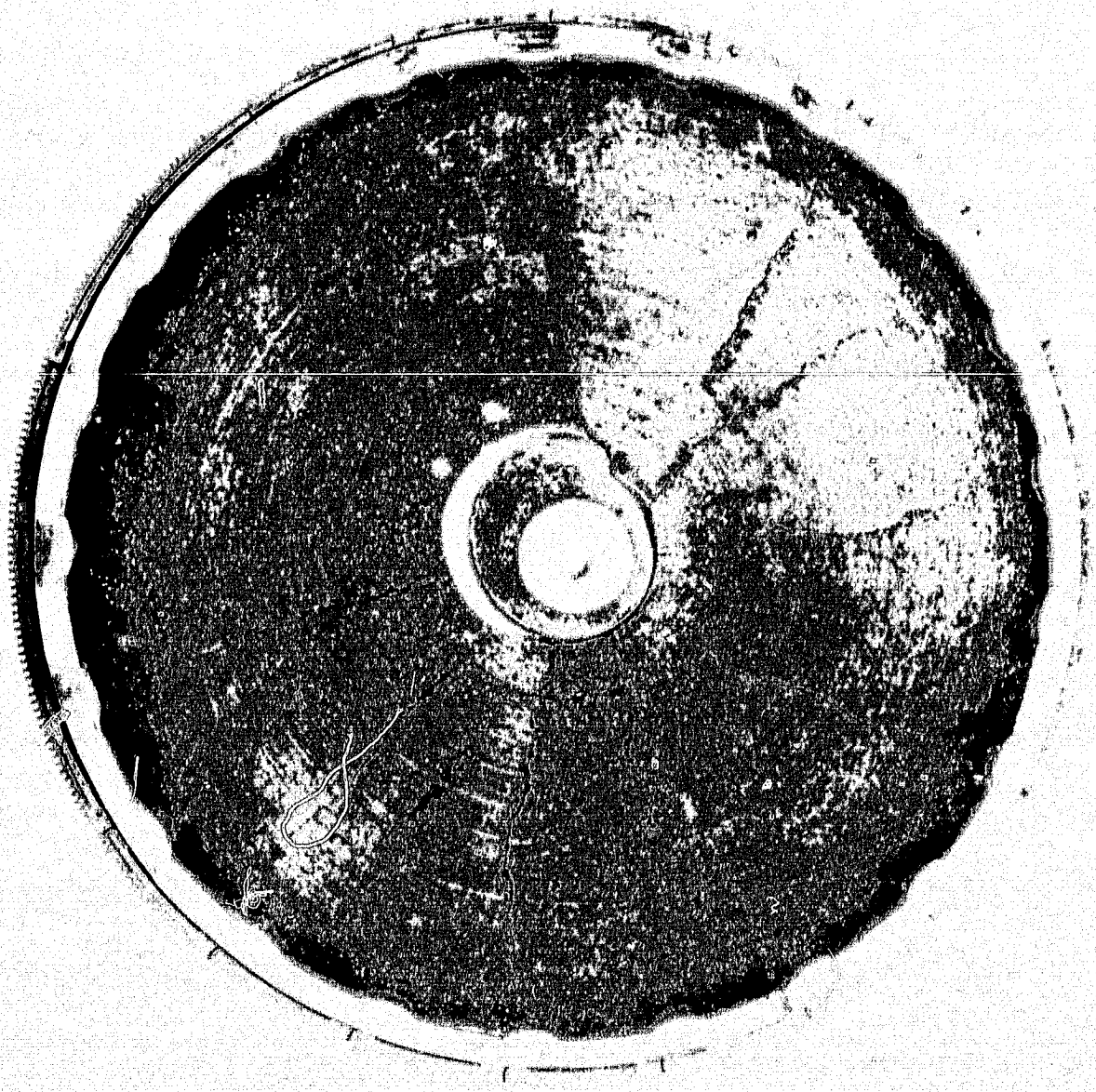

Figure 1.1.1 — Core Failure Caused by Chemical Attack

Since 1974 two materials, aluminum silicate (AS) and magnesium aluminum silicate (MAS), have been developed that are virtually impervious to chemical attack. This resistance to chemical attack has been demonstrated on full size cores in both accelerated and long-term engine durability tests. Five AS material cores have accumulated over 10,000 hours at 800°C (1472°F) in the 707 engine duty cycle. MAS cores have accumulated a maximum of 5000+ hours at this temperature.

In consideration of the high temperature requirements for future heat exchangers, three Ford 707 engines were specially modified to provide regenerator durability data at elevated temperature service. Seven AS regenerators have accumulated a total of over 27,000 durability test hours in these engines at average inlet temperature of 1000°C (1832°F). Of these, three cores accumulated over 5,000 hours and another 8,000 hours without thermal or chemical distress. The MAS regenerators have operated at 1000°C (1832°F) for a maximum of 500 hours so far. However, previous presented analysis[1] predicts that the MAS material is capable of prolonged operation at this temperature.

The majority of cores in use today in turbine and Stirling engines are made from these new materials. LAS cores can still be safely used in industrial waste heat recovery systems where sodium, potassium or sulphuric acid are not present in the exhaust products.

1.2 EXHAUST GAS ENVIRONMENT IN THE GAS TURBINE ENGINE

In the gas turbine engine, the regenerator is exposed alternately to the hot turbine exhaust and the relatively low temperature compressor discharge. The turbine exhaust consists primarily of the combustion products of the fuel and the intake air mixture. The combustion products of the diesel fuel used in the gas turbine engine are generally water vapor and carbon dioxide with minor amounts of sulphur dioxide. Oxides of nitrogen, zinc, vanadium, barium, calcium, sodium and other trace elements in the fuel are also present. There is sufficient mixing in the combustor and the turbine flowpath for the interaction of the various oxides to form other compounds, primarily sulphates and sulphuric acid vapor. The combustion air can contain significant amounts of ingested materials, depending upon the type of service conditions the engine is exposed to. In marine service applications significant amounts of salt in the form of salt water is ingested along with intake air. In road service applications minor amounts of fine dust, usually of clay and sand (silica and iron aluminum silicates) are ingested during normal operation, while ingestion of significant amounts of road salt is encountered in winter operation. Occasional contamination of the fuel with sodium bearing compounds have also been encountered. Although such instances are not common, accidental contamination is inevitable. In addition, oxidation and erosion products of the combustor, flow path and wear products from the seal system, bearings, etc. are also carried through the combustor. All these materials and the products of their interactions during combustion are potential corrosion agents acting on the heat exchanger. With the heat exchanger passages being very narrow and the surface temperatures being substantially lower than the exhaust gas for a considerable length of the heating cycle, condensation of the less volatile compounds can occur on the regenerator hot face as well as the passage walls. In addition, condensation of the sulphuric acid on the

porous walls near the cold face can also occur because of the temperature condition as seen in 707 engine operation. Thus the regenerator surface, including hot face and the passage walls, presents an active region for the condensation of various reaction products in the engine exhaust. The interaction of these condensed compounds with the matrix material is the source of chemical attack. The operating temperature of the regenerator significantly influences the type and amount of the condensate, as well as the reaction rates with the matrix materials.

All the test programs thus far have been aimed at evaluating the resistance of the matrix materials to the sodium ion attack (hot side) and sulphuric acid attack (cold side). These are perhaps adequate for 707 type heat exchanger environment (i.e., below 1000°C) since the corrosive action of the other constituents of the exhaust mentioned earlier may not be significant below 1000°C. Figure 1.2.1 illustrates the typical turbine exit and regenerator inlet temperatures for the Ford 707 gas turbine engine.

At higher temperature applications such as those encountered in the advanced gas turbine (AGT) engine, the influence of these compounds on matrix corrosion could be significant. For the AGT[2] application the turbine exit and regenerator inlet temperature requirements are illustrated on Figure 1.2.1.

At these temperatures, the oxides and/or sulphates of Fe, Zn, V, Mg, Na, Cu, etc., can form low melting compounds capable of severe fluxing action. Particularly Fe, V, Na and Zn ions could diffuse into the silicate structure to form low melting compounds. The fluxing action can be further aggravated by the presence of fluorides contributed by the wear of seal coatings.

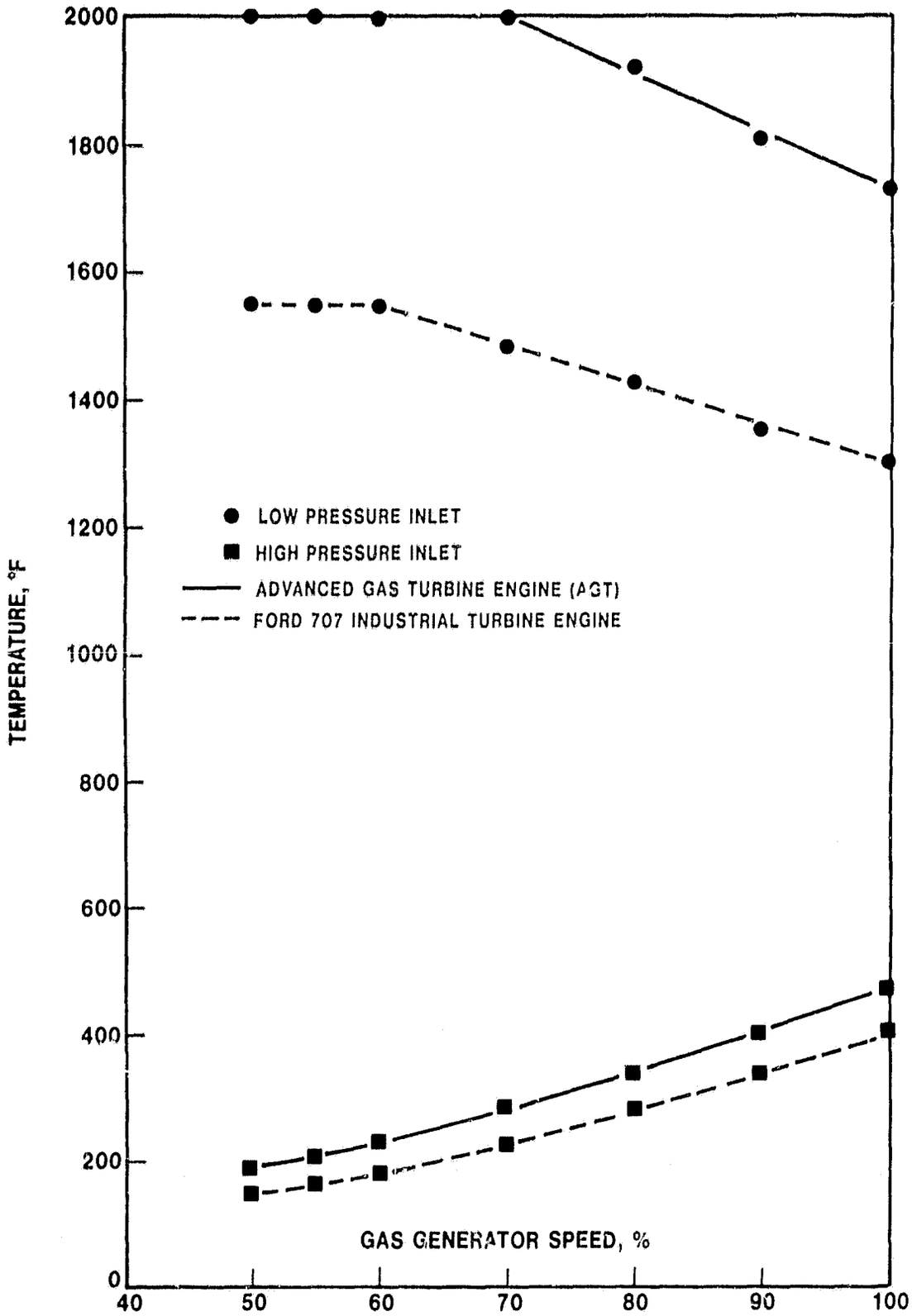

Figure 1.2.1 — Regenerator Inlet Temperatures Vs. Gas Generator Speed

1.3 STATUS OF OXIDE CERAMIC MATERIALS

While sufficient data exist which show that the AS and MAS materials are impervious to chemical attack in the Ford 707 engine (1000°C maximum regenerator temperature) the ultimate temperature limitations of these materials was not known. Laboratory tests were conducted to evaluate the operational capability of candidate oxide ceramic matrix materials at temperatures up to 1200°C.

The laboratory tests on the initial AS matrix specimens at temperatures up to 1200°C revealed some serious limitations with respect to the thermal stability and resistance to sodium attack at temperatures above 1000°C. At 1000°C, the thermal stability as well as the resistance to sodium attack (Fig. 1.3.1) appear marginal.

At 1050°, 1100° and 1200°C they are very poor (Figure 1.3.1). The current AS regenerators are made from the LAS matrix by leaching out all the lithium and subsequently heat treating the skeletal β spodumene structure to partially sinter and strengthen the matrix. This structure is inherently unstable and will ultimately convert to AS keatite/mullite structure. The rate of this transformation is a function of temperature and can occur very rapidly at temperatures 1000°C and above. This phase transformation results in a change in cell dimensions, as has been observed in the 1100° and 1200°C thermal instability test, as well as a change in thermal expansion. Although no sodium ion attack is observed below 1000°C, above this temperature the sodium appears to diffuse rapidly into the lattice forming low melting silicate compounds. At temperatures above 1100°C, these reactions are so rapid that severe fluxing of the AS matrix occurred in a very short time.

A second generation AS material with potential for improved thermal stability up to 1100°C has recently been received for evaluation in the laboratory as well as engine testing. The upper temperature limit for this material will be established by subsequent testing.

The current MAS matrix materials, being of the cordierite type with the Mg ions tightly bonded to the silicate structure, are highly stable and are more resistant to ion exchange. Properly fired MAS matrices have demonstrated thermal stability and excellent resistance to sodium ion attack at temperatures up to 1200°C (Figs. 1.3.2 & 1.3.3). The MAS matrices tested are made by two different processes from two types of raw materials, namely mineral base and glass frit base. For the mineral base MAS the starting materials are primarily clay and talc, with the composition adjusted to yield cordierite ($MgO:Al_2O_3:SiO_2$—2:2:5) in the fired structure by the addition of alumina and silica. This type of matrix is usually porous but of lower thermal expansion. For the glass-ceramic, the starting material is a glass-frit powder of primarily MAS-2:2:5 composition with minor amounts of nucleating agents. The firing cycle is such that glass sinters and crystallizes more or less completely during firing. Very high wall density and high strengths are achieved with this material, however, the thermal expansion is usually slightly higher than the mineral base MAS matrix. The source of thermal instability in both types is usually the transfor-

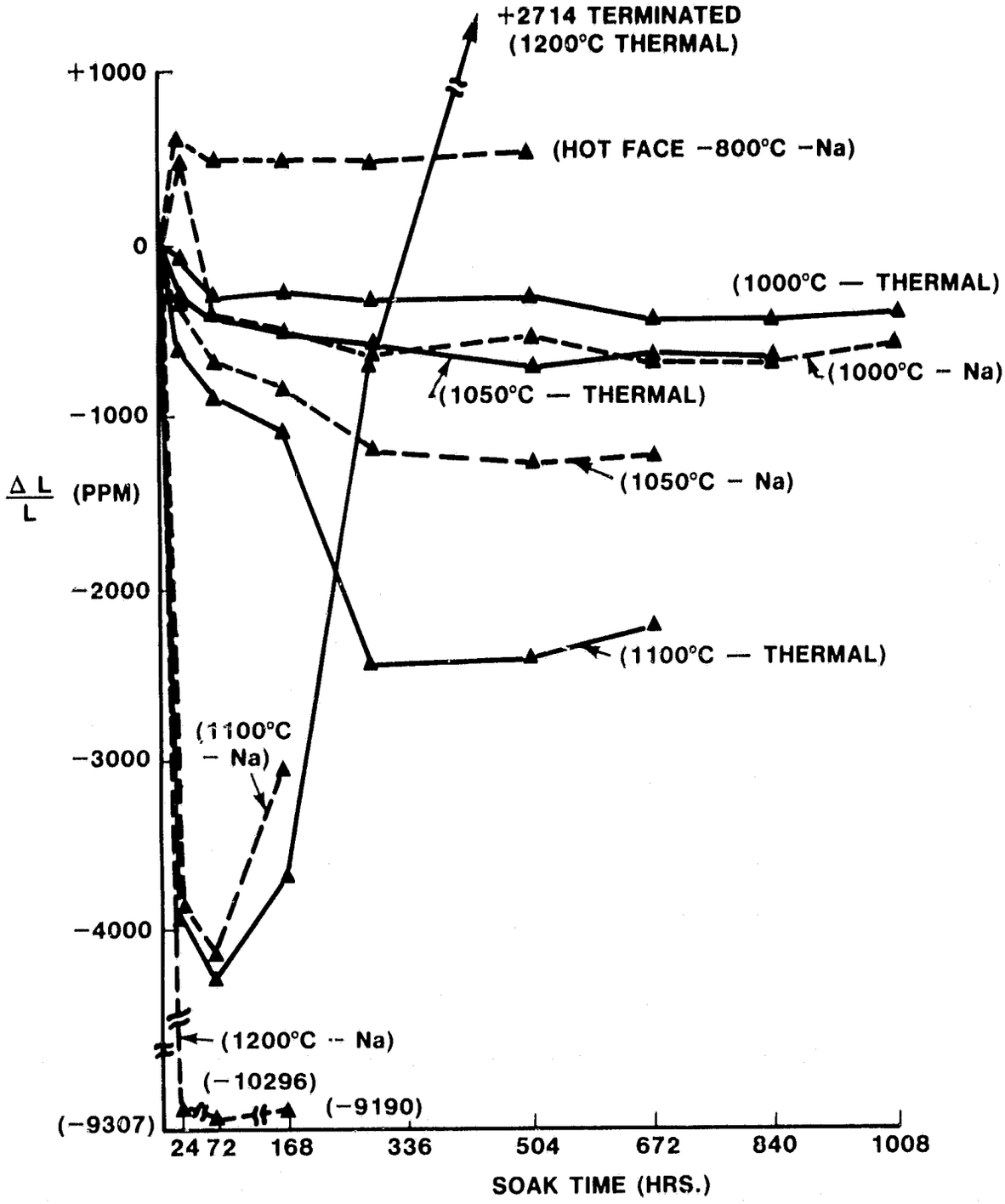

Figure 1.3.1 — Supplier A, AS; Thermal Stability With and Without Sodium at 800°C to 1200°C.

mation of the residual glass phase in the fired matrix. This can, however, be removed by appropriate heat treatment prior to service installation. The glass frit base matrix demonstrated excellent resistance to chemical attack (Fig. 1.3.2). The mineral base matrix (Fig. 1.3.3) though not as good as that of the glass frit base, is still adequate up to 1200°C.

At the present time test data that can systematically evaluate the influence of oxides and/or sulphates of Fe, Zn, V, Mg, Na, Cu, etc., which can form low melting compounds capable of severe fluxing action, on these matrix materials at temperatures up to 1200°C is non-existent.

In summary, it appears that the current AS and MAS oxide ceramic materials can perform adequately in the regenerator application of the "state-of-the-art" gas turbine engines (up to 1000°C). For higher temperature applications, such as the AGT, the AS material, which has desirable low thermal expansion characteristics, must demonstrate improved thermal stability and resistance to chemical attack at temperatures up to 1100°C. The second generation AS material, which is presently being evaluated, may satisfy this requirement. Further development of this material would be required for 1200°C applications.

Based on laboratory testing up to 1200°C, the current MAS materials offer the potential for adequate thermal stability and resistance to chemical attack up to 1200°C application. However, due to the much higher thermal expansion characteristics of the MAS compared to AS materials, they will require extensive design modifications to accommodate the increased thermal stresses, which will be discussed in a subsequent section.

For these reasons silicon nitride, which is believed to have higher temperature capability, is being considered for 1200°C applications. The next four sections will examine this material with regards to physical properties, manufacturing feasibility, thermal stress and aerothermodynamic performance.

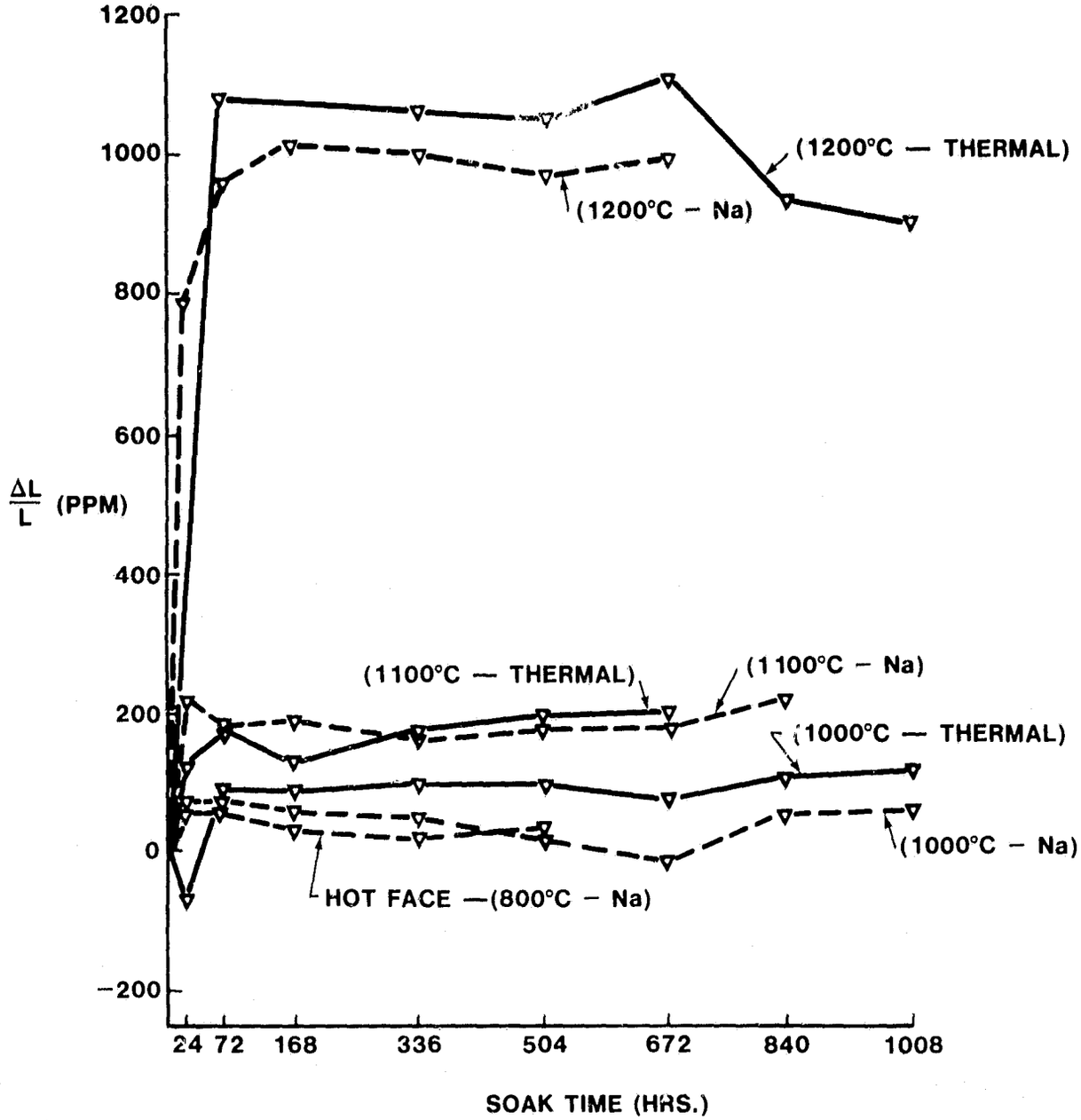

Figure 1.3.2 — Supplier K, MAS Glass Frit; Thermal Stability With and Without Sodium at 800°C to 1200°C.

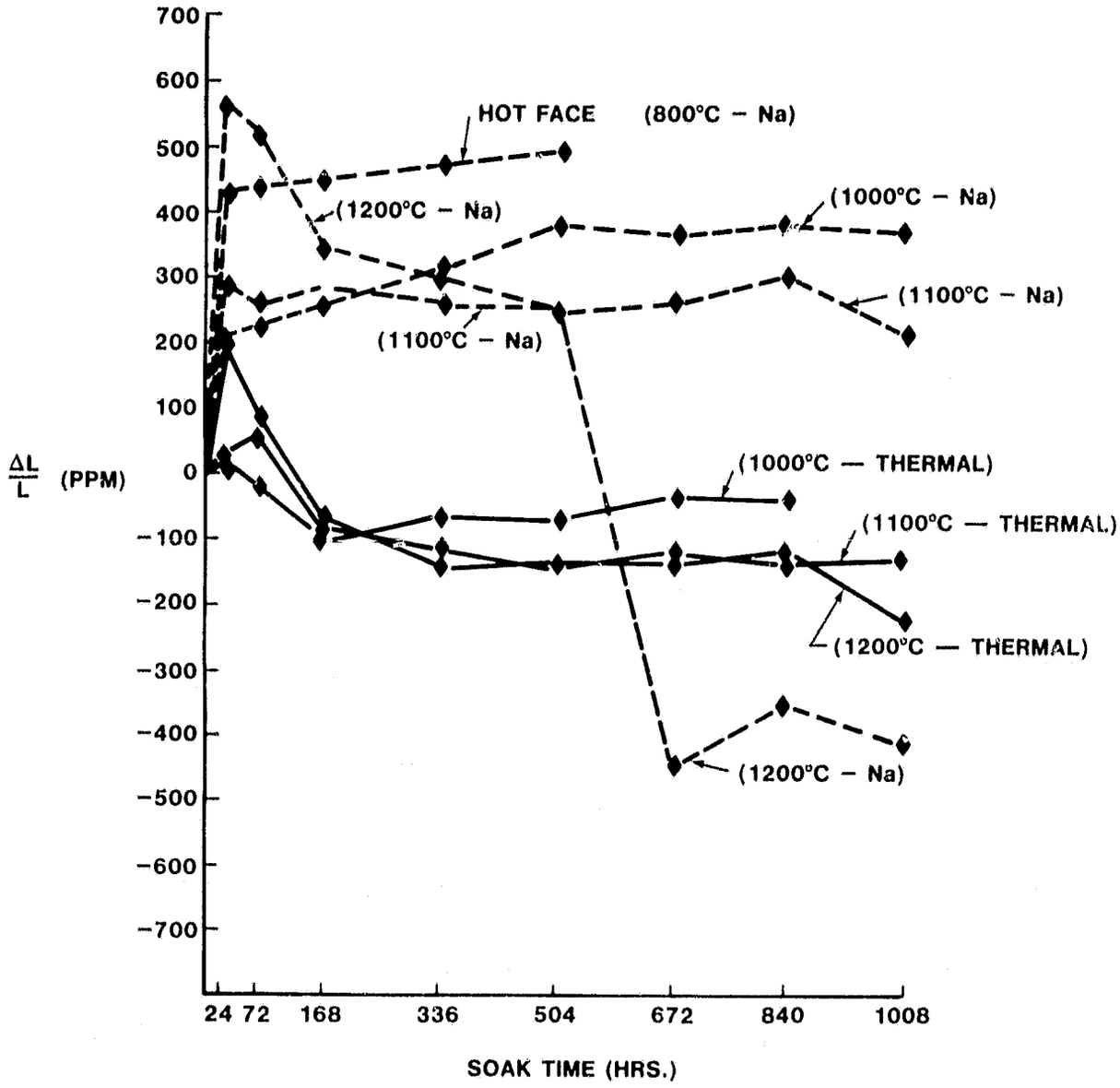

Figure 1.3.3 — Supplier G, MAS Mineral Base; Thermal Stability With and Without Sodium at 800°C to 1200°C.

2.0 SILICON NITRIDE MATERIAL PROPERTIES

2.1 INTRODUCTION

Silicon nitride provides certain definite advantages with respect to the manufacture and physical properties of the regenerator matrix. The manufacturing aspects will be discussed in a later section. The functional advantages of the silicon nitride matrix are as follows:

Silicon nitride has much higher temperature potential than the state-of-the-art oxide base matrix materials. This provides added protection against melting and glazing caused by rapid burning of fuel condensed on the regenerator surface during flame-outs.

The nitriding reaction does not produce intermediate phases. This enables the firing of large matrices with section thickness variations without residual stresses or crack problems which are unavoidable in the LAS and MAS firing. This permits the regenerator design to include complex passage geometries and varying section thicknesses, which is not possible with the oxide base regenerators.

There is little or no shrinkage during firing which permits the control of wall density and porosity by the judicious selection of the starting silicon powder particle size distribution. This allows the specification of wall surface characteristics desirable for optimum heat transfer in regenerator passage design.

There are, however, certain disadvantages expected with the silicon nitride matrices. These are:

Higher theoretical density material (3.18 for Si_3N_4 vs. 2.51gm/cc for MAS) which increases the mass of the regenerator with attendant additional stresses on the regenerator drive system

The existing test data indicate certain problems with respect to thermal stability, oxidation resistance and resistance to chemical attack in salt bearing engine exhaust environment.

These issues will be discussed in some detail.

2.2 THERMAL STABILITY

The early in-house work on the reaction bonded silicon nitride (RBSN) material pointed out serious deficiencies with respect to thermal stability in thick sections. The problem apparently was due to residual silicon. In case of thick sections or inadequate firing cycles significant amounts of silicon remains unreacted due to insufficient nitrogen availability. The residual silicon oxidizes in service at high temperature in air and the resulting volume change produces growth in the part.

The oxide formation also results in a change in thermal expansion. In addition, significant loss in strength results from the cracks generated due to stresses produced by the volume change when Si is oxidized to SiO_2. Porosity and inherently large surface area in regenerator matrices permit rapid diffusion of oxygen. Rapid deterioration of matrix physical properties has been observed even with only a small amount of residual silicon at temperatures as low as 900°C.

More recent work[3] on the RBSN reported significant improvement in the firing cycles yielding nearly complete reaction with little or no residual silicon. Thermal stability of RBSN matrices fabricated utilizing the improved firing cycles is in the range of that of the current MAS matrices at 1200°C. Strength loss after 200 hour exposure to 1200°C in air is also relatively small.

2.3 OXIDATION RESISTANCE

In the early work the oxidation resistance of the RBSN was indicated to be very poor, evidently, due to residual silicon. Significant weight gain at 900°-1200°C were observed accompanied by a strength loss in excess of 30% in many cases. More recent work showed that specimens produced by the improved firing cycles that contain little or no residual silicon, the oxidation rates and strength losses after prolonged exposure to 900°-1200°C were too high. It has been observed that the silicon nitride decomposes in air as represented by the reaction $Si_3N_4(S) + 3O_2(g) \rightarrow 3SiO_2(S) + 2N_2(g)$ with the standard free energy as high as −1700KJ/mole in the 1000°-1400°C range[4]. The silicon nitride is unstable with respect to SiO_2 and the reaction rate is controlled by the availability of oxygen. Investigations[5,6] dealing with the oxidation mechanisms in silicon nitride demonstrated that the diffusion of oxygen through the oxide layer to the silicon nitride/oxide interface controls the oxidation rate. In the 900°-1200°C range the oxidation rates are not rapid enough to produce a tenacious oxide layer and the oxide film formed tends to be porous and cracked due to the evolution of nitrogen gas. Diffusion of oxygen through this type of oxide layer is quite rapid and the oxidation rates are very high. At temperatures above 1300°C the initial oxidation rates are very high, promoting the formation of a dense tenacious oxide layer on the silicon nitride surface. Once a dense oxide layer is formed the oxidation rate is drastically reduced because of the very slow diffusion of oxygen through the dense silica layer. At these temperatures the oxidation rate approaches the typical parabolic oxidation representing the diffusion of oxygen through solid silicon dioxide. Surface treatments taking advantage of this phenomena that yield acceptable oxidation rates in the 900°-1200°C range are now available.

2.4 RESISTANCE TO CHEMICAL ATTACK

Since silicon nitride is an important candidate material for the flow path component application in the advanced gas turbine engines, hot corrosion of silicon nitride has been the subject of several investigations[6,7,8,9]. These investigations involved the study of hot corrosion of silicon nitride in simulated combustion products of diesel fuel and high Na and S bearing residual oil as well as accelerated corrosion in salt and oxide environment. All these investigations confirm that a

stable protective silicon dioxide layer is essential for the oxidation resistance in the exhaust gas environment. The exhaust gas environment resulting from the burning of clean diesel fuel (<1 ppm Na and .5% S) produces no serious hot corrosion effects on silicon nitride bars in the 900°-1400°C range[8]. Accelerated corrosion tests with oxides of vanadium, primarily V_2O_5, showed that these oxides, which are known to cause severe corrosion on stainless steels and superalloys, have no harmful effect on RBSN. When sodium sulphate is added to the V_2O_5, severe corrosion was observed in the 900°-1300°C range. This latter condition simulates the hot corrosion effects of the condensate from combustion products of residual oil (50 ppm Na and 50 ppm V). Sodium ion bearing salts, e.g. NaCl and $NaSO_4$ with or without the presence of V_2O_5 caused a drastic increase in the oxidation rate of silicon nitride in the 900°-1350°C range. The salts produce severe hot corrosion in vapor as well as condensed states. The corrosion is particularly severe in the condensed state, i.e. approximately 1100°C temperature range[8]. Since the heat exchanger matrices are of characteristically high surface area to volume ratio they present a very large reaction surface. The wall porosity, which is significant, presents a considerable amount of additional surface for condensation as well as reaction. The hot corrosion effects of the salts in the combustion products, therefore, pose serious concerns for the application of silicon nitride for the heat exchanger application. In view of the possible exposure of the silicon nitride matrices to sodium bearing salts in service, it is important to understand the hot corrosion mechanisms so as to be able to explore possible solutions.

An insight into the actual oxidation-corrosion processes in RBSN in the presence of NaCl and Na_2SO_4 in oxidizing environment is provided in References 6, 8 and 9. Oxidation resistance is provided by the formation of a protective silicon dioxide film as discussed earlier by the reaction:

$$Si_3N_4\ (s) + 3O_2(g) \rightarrow 3SiO_2(s) + 2N_2\ (g)$$

The oxidation rate is controlled by the diffusion of oxygen through the silicon dioxide layer when a tenacious and dense film is present. The oxidation rate corresponds to the diffusion of oxygen through solid silica and therefore is a function of the film thickness and the active diffusion surface area.

In presence of sodium sulphate and sodium chloride the protective oxide layer on the silicon nitride surface is unstable and is removed as per the reactions:

$$Na_2SO_4(l) + 2\ SiO_2(s) \rightarrow Na_2SiO_3\ SiO_2(l) + SO_3(g)$$
$$Na_2SO_4(l) + SiO_2(s) \rightarrow Na_2SiO_3(l) + SO_3(g)$$
$$2NaCl\ (l) + SiO_2(s) + 1/2\ O_2(g) \rightarrow Na_2SiO_3(l) + Cl_2(g)$$

These reactions involving the salts in the condensed state are valid up to 1100°C above which the salts will be in gaseous state and reactions involving the salts in vapor form will prevail. The interaction of salts with the silica layer results in the formation of a film of liquid sodium silicate. Silica is soluble in sodium silicate, and the silica film dissolves in the sodium silicate until reaching the saturation point. In the presence of excess quantities of the salts, as expected to be the case with the

regenerator deposits, the silicon in the liquid sodium silicate reacts with the salts producing additional amounts of sodium silicate. The resulting depletion of silica from the sodium silicate layer combined with the formation of additional amounts of the sodium silicates insures the continuous removal of silica layer from the silicon nitride surface. Thus at temperatures 1100°C and below the formation of protective oxide layer on the silicon nitride surface is prevented. The diffusion rates of oxygen through the liquid sodium silicate layer is significantly higher than that through solid silica film. Thus in the absence of the protective silica film the oxidation rate of silicon nitride approaches that corresponding to the diffusion rate of the oxygen through liquid sodium silicate. The oxidation rate increases rapidly as the temperature reaches 1100°C and the hot corrosion is expected to be severe in the 1100° temperature range.

At temperatures above 1100°C the salts are in vapor state and are not expected to condense on the regenerator surface. The reactions involving the salt vapor and silica are essentially the same as those mentioned earlier. Once a stable layer of sodium silicate is formed, however, the reaction kinetics are quite different. The silicon nitride oxidation is controlled by the diffusion of oxygen through the sodium silicate layer to the silicon nitride surface which becomes increasingly rapid as the temperature increases. Since the salts are in vapor state, silica film dissolution now is controlled by the diffusion of sodium oxide from the sodium salt vapor to the silica layer through the liquid sodium silicate film. Thus the stability silicon dioxide film is now controlled by the concentration of sodium oxide in the sodium silicate layer which is a function of salt vapor concentration in the environment. At high temperatures, e.g. above 1200°C the diffusion of oxygen through sodium silicate is very rapid producing a thick oxide layer on the silicon nitride surface. The diffusion rate of oxygen through the sodium silicate at these temperatures is apparently high enough to maintain a stable oxide film in an environment consisting of air saturated with sodium sulphate vapor[9]. Once a stable oxide layer is formed the oxidation rate of silicon nitride is controlled by the diffusion of oxygen through the silicon dioxide layer to the silicon nitride surface. At temperatures above 1300°C, as discussed earlier, the oxidation of silicon nitride tends to produce an impervious oxide film at the silicon nitride surface accompanied by a significantly lower oxidation rate. The stability of the silica film is now governed by whether or not the lower rate of diffusion of oxygen through the silica film to the silicon nitride surface is adequate to replenish the silicon dioxide dissolved from the film surface. The work cited showed that a stable oxide film is formed above 1350°C in air saturated with NaCl and Na_2SO_4 vapor. The hot corrosion rates in salt vapor decreased rapidly with increasing temperature in 1250°-1400°C range and were significantly lower than the hot corrosion rate in liquid sodium sulphate at 1100°C. Limited test data available on CVD silicon nitride indicated that this form of silicon nitride, because of its nearly theoretical density, yields superior oxidation-corrosion resistance.

To summarize,

Silicon nitride with appropriate surface treatments can perform with adequate oxidation resistance at temperatures up to 1350°C in the gas turbine exhaust consisting of combustion products of clean diesel fuel (<1 PPM Na and .5% S).

On the basis of the evidence presented, it is believed that the hot corrosion resistance of the silicon nitride in turbine exhaust containing large amounts of metal oxides and sodium salts (e.g. combustion products of residual oil with 50 PPM Na and 3% S) may be adequate at temperatures above 1350°C and possibly in the 1200°-1350°C range. At temperatures 1100°C and below where the sodium salts are in condensed (liquid) state the hot corrosion effects are very severe.

In the regenerator application, where the temperatures range from 100°C on the cold side to 1200°C on the hot side, the enormous amount of reaction surface presented by the inherently high surface to volume ratio will result in condensation and accumulation of salts. Severe hot corrosion and deterioration of the silicon nitride matrix are expected in marine service and winter road service.

The silicon nitride matrices can be expected to perform adequately at temperatures up to 1350°C regenerator application in turbine engines burning clean sodium free fuel, however, are not considered suitable for automotive application unless appropriate surface treatments are developed to prevent the attack of condensed salts at 1100°C.

3.0 MANUFACTURING PROCESSES

3.1 REACTION BONDED SILICON NITRIDE

There are several processes available for the fabrication of silicon nitride components, e.g. hot pressing, reaction sintering, or reaction (RBSN) bonding, chemical vapor disposition (CVD), etc. Of these, only the reaction sintering (RBSN) appears to be suitable for the fabrication of regenerators because of the thin walls and the complexity of the matrix structure. In the RBSN process, silicon powder of appropriate characteristics is compounded with a suitable binder, formed into the desired shape by an appropriate means — such as injection molding or extrusion followed by firing in nitrogen to remove the binder and reaction sinter in nitrogen or nitrogen-hydrogen mixture to produce silicon nitride. The firing cycles are carefully designed to produce complete conversion of silicon to silicon nitride and the setting and furnace arrangement are such that a uniform distribution of the nitrogen throughout the part is ensured.

This process is readily adaptable to the various methods[10] used for the fabrication of regenerator matrices, particularly calendaring and extrusion. Processes capable of yielding matrices of .004″ material wall thickness utilizing both calendaring and matrix extrusion have been developed and the fabrication of silicon nitride regenerators is believed feasible.

3.2 COST CONSIDERATIONS

Although the cost aspects of the silicon nitride regenerator are not yet well defined, an attempt will be made to provide a comparison of the manufacturing aspects of the silicon nitride and the MAS regenerators. This is considered appropriate since the MAS regenerator appears to be the most promising candidate for automotive gas turbine application for 1200°C service and also appears to be the least expensive of the state-of-the-art oxide base regenerators. In order to be competive, the cost of the silicon nitride regenerator should be comparable to that of a MAS regenerator for a similar application. A recent cost study[10] established that the extruded MAS regenerator matrix provides the least expensive regenerator.

The cost of the raw materials used in the manufacture of silicon nitride regenerators and MAS glass-frit regenerators are comparable, e.g. 45-60¢ for Si powder vs. 40-75¢ for MAS glass-frit/lb. The clay talc powder used for the mineral base MAS regenerators, however, is considerably cheaper (approx. 20¢/lb.)

The nitriding reaction, i.e. the conversion of Si to Si_3N_4, produces a 60-64% weight gain accompanied by little or no shrinkage in the fired parts. This is in contrast to the 8 to 20% firing shrinkage encountered with MAS matrices. The absence of firing shrinkage in silicon nitride matrices virtually eliminates all scrappage caused by the shrinkage cracks (as much as 30% in case of MAS matrices) resulting in very high yields. It is, therefore, expected that the material costs on per finished unit basis are expected to be favorable for the silicon nitride regenerators even though the initial raw material costs are higher.

For the calendaring process the fabrication costs are expected to be equivalent for both silicon nitride and MAS, since the basic process steps are almost identical.

In the case of matrix extrusion, however, the process cost for silicon nitride are expected to be lower. The die costs for the extrusion of thin wall (0.004" wall thickness) matrices are expected to be significantly lower with the soft metallic silicon when compared to the highly abrasive MAS powder.

Since there is no shrinkage during firing, the silicon nitride matrices are usually free of residual stresses and shrinkage cracks. The absence of stresses during firing permits the fabrication of large regenerators by bonding together smaller sections in the green state followed by firing. This makes it possible to utilize smaller dies and smaller extruders resulting in significantly lower equipment costs. The die costs as well as the equipment costs rise very rapidly with the increase in size of the extrudite. Conversely, the MAS regenerators have to be made either in one piece or by assembling fired segments with a high temperature adhesive. To obtain adequate strength at the joints, the assembled regenerator might have to be refired, which would incur an additional cost increase. Such a regenerator may not be as reliable as a one piece matrix.

Since there is little or no shrinkage during firing for silicon nitride regenerator matrices, all the sizing and major machining operations can be performed in the green state with only minor finishing after firing. This results in substantial savings in the regenerator cost. Due to the high firing shrinkage associated with the MAS regenerators all the machining operations have to be carried out after firing. Since MAS is very hard (e.g. cordierite glass-ceramic is as hard as quartz), expensive diamond grinding is required for all sizing and machining operations.

In the case of firing large regenerators such as the Ford 707 regenerator, elaborate settering is required to absorb firing shrinkage. When the firing involves the formation of intermediate phases that have characteristics, which are significantly different from those of the starting and final phase, as is the case with MAS, the temperature distribution must be uniform to avoid localized stresses and possible cracking. The settering also should be designed to allow drag free movement. These factors account for a significant part of the regenerator firing and handling cost. Because of the absence of firing shrinkage and intermediate phases, the settering and handling costs during firing are expected to be much lower for silicon nitride matrices.

The nitriding reaction, i.e. the conversion of Si to Si_3N_4 is an exothermic reaction. The rate of reaction and therefore the rate of heat evolution are controlled by the availability of the nitrogen in the reaction zone. An uneven nitrogen distribution in the matrix can produce localized fast reaction zones. In these areas, the excessive heat generated can melt the unreacted silicon, and thus block off the passages for nitrogen flow. This results in significant amounts of residual silicon. Since the nitrogen diffuses from the outer skin to the center of the part, unduly rapid reactions at the skin can block off the access of nitrogen to the silicon in the interior. This also results in the presence of undesirable residual silicon. It is therefore very important to develop firing cycles capable of complete and even reaction

excessive heat generated can melt the unreacted silicon, and thus block off the passages for nitrogen flow. This results in significant amounts of residual silicon. Since the nitrogen diffuses from the outer skin to the center of the part, unduly rapid reactions at the skin can block off the access of nitrogen to the silicon in the interior. This also results in the presence of undesirable residual silicon. It is therefore very important to develop firing cycles capable of complete and even reaction throughout the part. Currently available firing cycles are capable of accomplishing this. These cycles, however, are too long as they are designed for structural parts with large section thickness and are therefore too expensive. It is believed that economical firing cycles can be developed for silicon nitride since diffusion thicknesses involved are less than .002" and the binder burn-out leaves sufficient pore volume for the nitrogen diffusion throughout the passage walls.

The cost considerations discussed thus far do not include surface enhancement treatments required to improve resistance to chemical attack. In the event these treatments become essential for attaining durability objectives, they must be included in the final regenerator matrix cost. At this time chemical vapor disposition (CVD) is a process that appears promising for improving chemical attack resistivity. Unfortunately, the CVD process is also very expensive. Consequently, a more economical surface enhancement treatment appears to be required to ensure the cost effectiveness of a silicon nitride regenerator for application environments involving chemical attack.

In summation, on the basis of raw material, fabrication, firing and machining costs, it appears that the silicon nitride regenerators can be readily mass produced at a cost competitive with those of the oxide base (e.g. MAS) regenerators. It should be recognized, however, that additional process steps such as CVD to make the passage walls impervious to oxidation and chemical attack can add to the cost of the silicon nitride regenerators significantly. This factor will ultimately determine the cost effectiveness of a silicon nitride regenerator.

4.0 THERMAL STRESS

Thermal stress is one of the major factors which must be considered in order to develop a durable regenerator. The typical rotary heat exchanger has relatively cool air surrounding its rim, while hot gases pass through its interior. In effect this constitutes a hot interior cylinder being restrained by a cooler cylinder that is equivalent to the width of the peripheral rubbing seals. The highest tensile stress occurs at the outside diameter on the hot face and rapidly changes to a compressive stress in the hot central portion of the core below the peripheral seal inner diameter as illustrated on Figure 4.1. Thermal stress in AS heat exchangers would be significantly lower than those in MAS or silicon nitride regenerators primarily due to the low thermal expansion characteristics as illustrated on Figure 4.2.

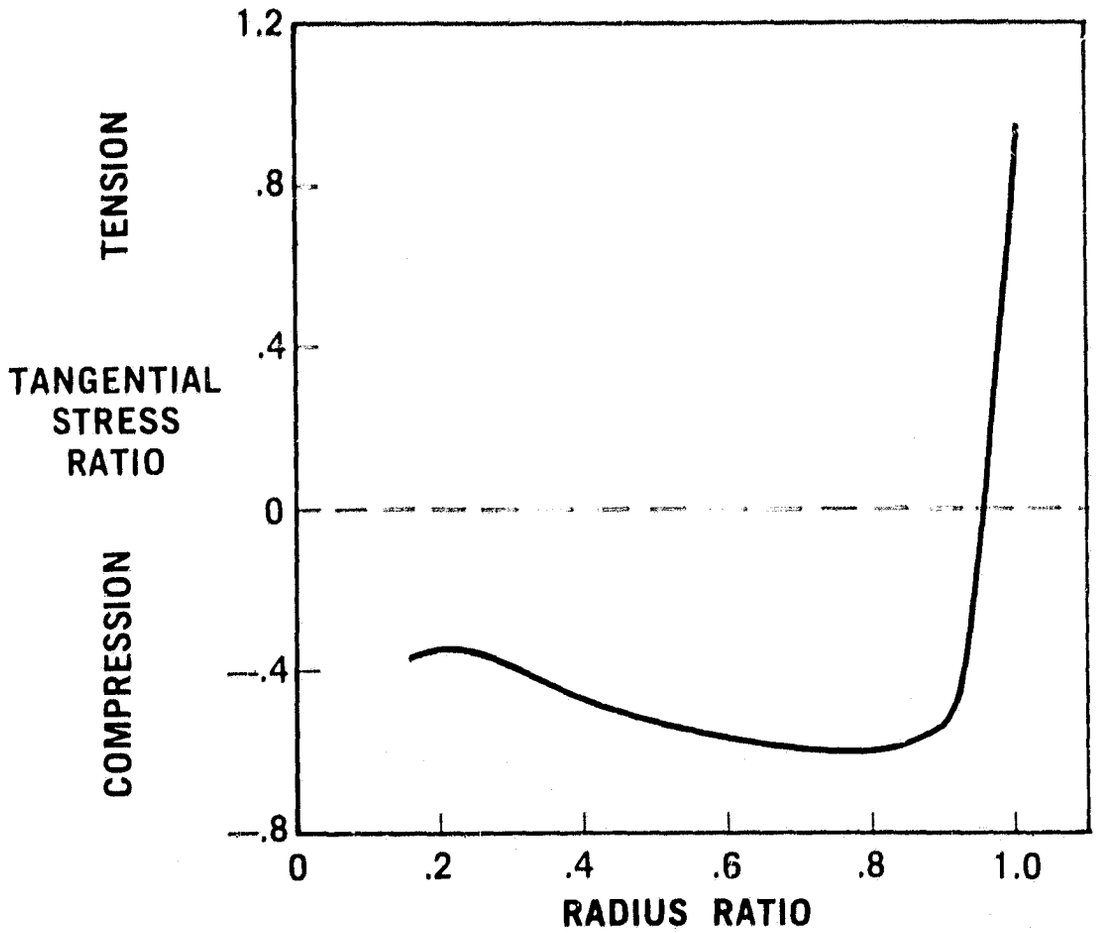

Figure 4.1 — Tangential Thermal Stress Distribution at Regenerator Hot Face

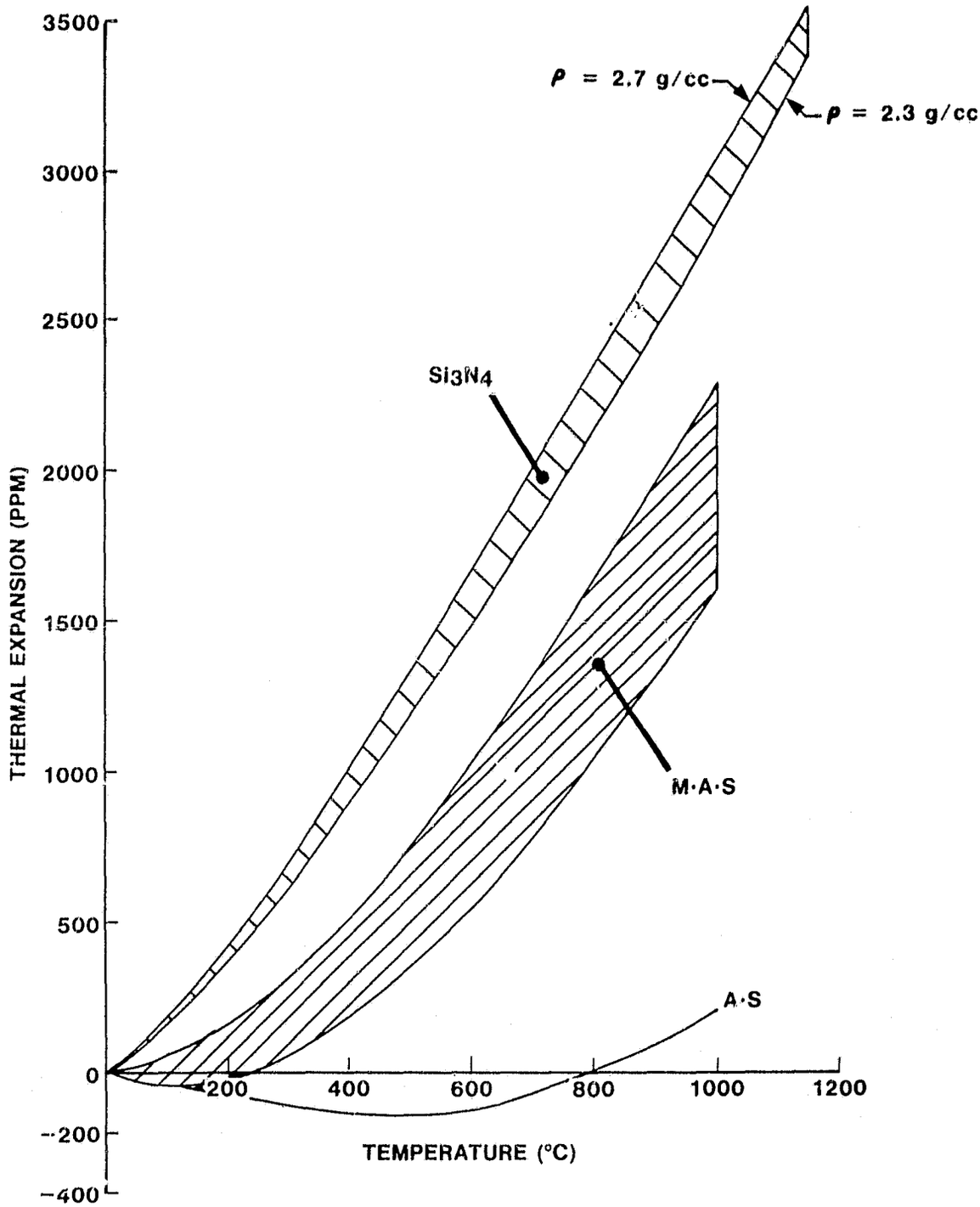

Figure 4.2 — Thermal Expansion Characteristics of Various Materials

Although past experience has shown that mechanical loads imposed on the matrix through the seal and drive system cannot be overlooked, the primary operating stress is thermal. Assuming the matrix material properties are not altered adversely due to chemical attack or thermal instability during engine operation, thermal stress failure will not occur provided the regenerator has an adequate thermal stress safety factor. Thermal stress safety factor (S.F.) is defined as the ratio of the core matrix modulus of rupture (MOR), as determined by a four point bend test, to the maximum calculated thermal stress ($\sigma_{T_{MAX}}$). MOR is a measurement of overall matrix condition and is dependent not only on material strength, but bond integrity and cell geometry as well.

Another important parameter for thermal stress capacity is the matrix strain tolerance. Strain tolerance (S.T.) is defined as the ratio of modulus of rupture (MOR) to modulus of elasticity (MOE) of the matrix. Since thermal stress is proportional to MOE, maximum values of strain tolerance are desirable for improving thermal stress capacity. In other words, thermal stress safety factor can also be defined as the ratio of matrix strain tolerance to the maximum calculated thermal strain ($\epsilon_{T_{MAX}}$).

Once the thermal stress safety factor has been defined for a given matrix material configuration, the designer has limited flexibility for improvement. The most effective approaches for safety factor improvement are as follows:

1. Increase the ratio of matrix outer radius to peripheral seal inner radius.

2. Reduce the tangential elastic modulus at the rim with respect to the elastic modulus below the peripheral seal inner radius.

3. Incorporate stress relief techniques at the rim.

4. Impose a radial compressive preload at the rim.

By increasing the width of the peripheral seal at the rim, which increases the ratio of matrix outer radius (R_O) to peripheral seal inner radius (R_S), the radial thermal gradient at the hot side rim is effectively reduced. Figure 4.3 illustrates the potential reduction of thermal stress level irrespective of the actual regenerator size.

Figure 4.4 illustrates maximum thermal stress at the rim (R_O) is primarily proportional to the ratio of tangential elastic modulus in the rim ($R > R_S$) to the modulus of elasticity below the inner seal radius (R_S). In order to accomplish this, the fabrication process must be able to alter the matrix geometry between the inner seal radius (R_S) and core outer radius (R_O) to increase the matrix strain tolerance in this region. By reducing the MOE at a faster rate than the MOR, S.F. can be increased substantially.

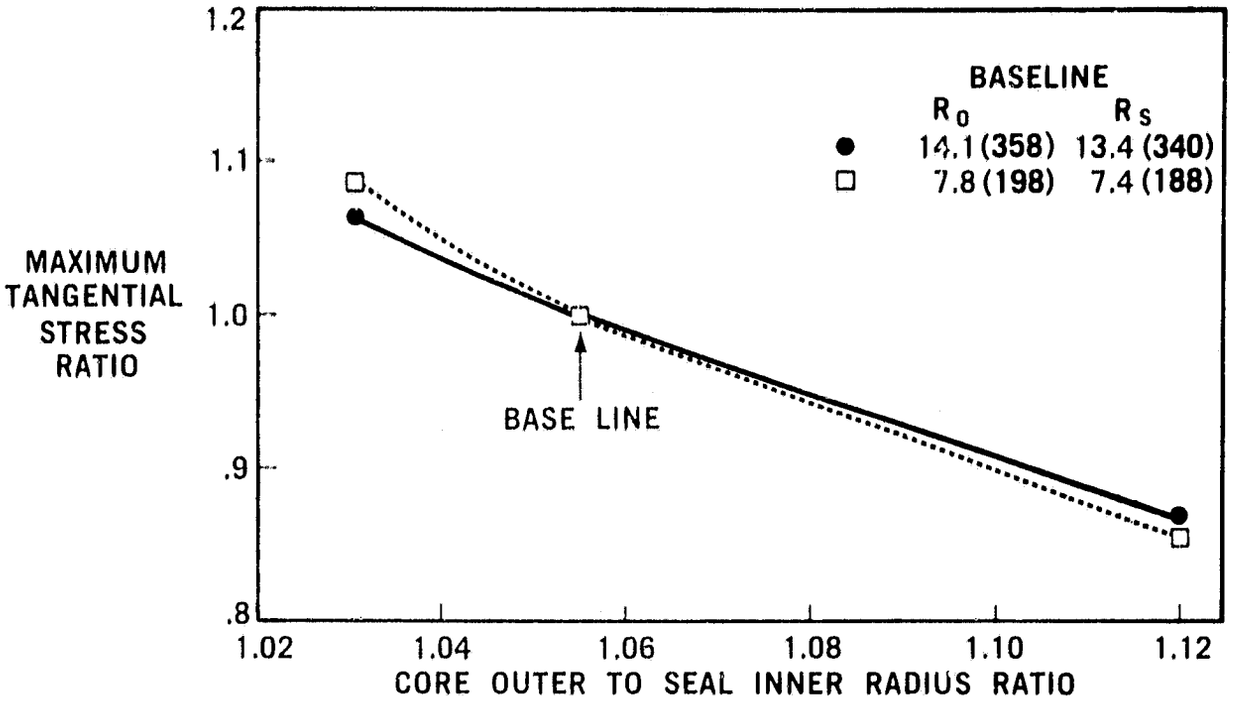

Figure 4.3 — Maximum Tangential Stress Ratio Vs. Regenerator Outer to Seal Inner Radius Ratio

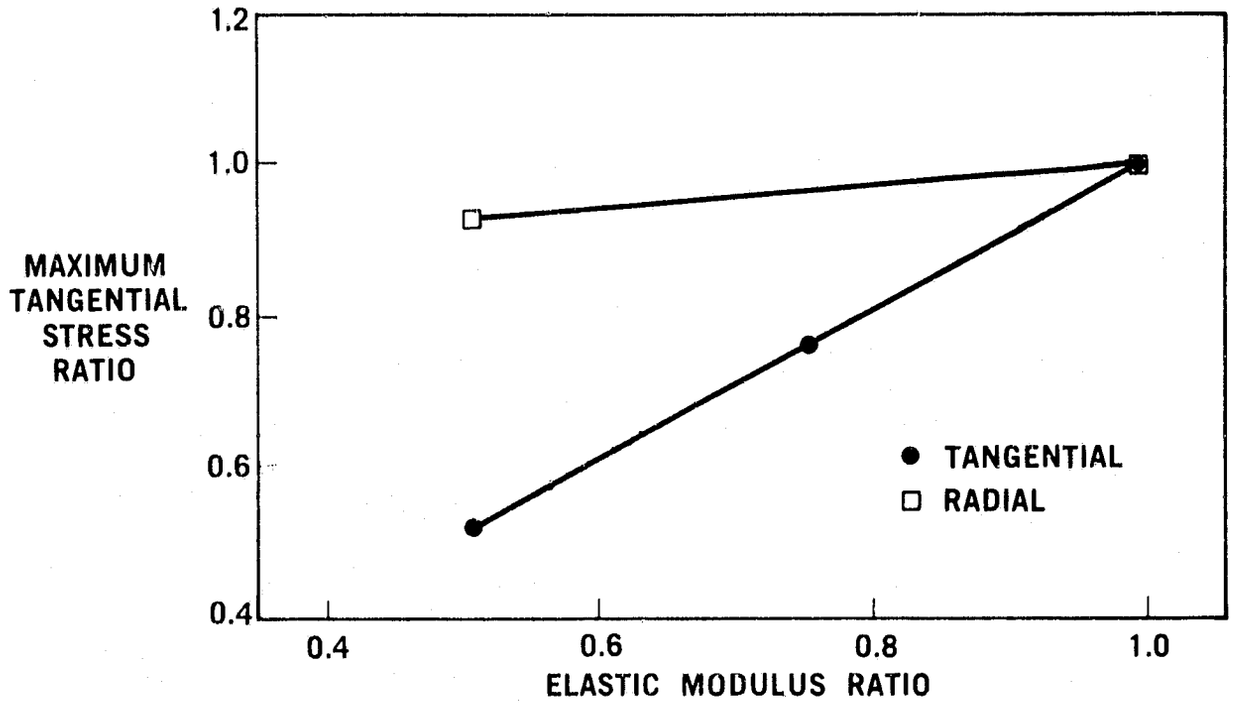

Figure 4.4 — Maximum Tangential Stress Ratio Vs. Elastic Modulus Ratio

In many cases, the thermal stress safety factor of a regenerator can be improved by the addition of stress relief slots in the rim. A typical stress relieving scheme used on high thermal expansion cores, where the critical stress is tangential tension in the rim, consists of a number of narrow slots extending radially to just below the peripheral seal I.D. on the regenerator hot face, and tapered axially from the seal I.D. to the middle of the rim as shown in Figure 4.5. These slots are filled to prevent leakage.

Another method of increasing the thermal stress safety factor is by introducing a compressive load at the rim to interact with operating tensile thermal stresses. This is accomplished in the Ford regenerator by elastomerically bonding the ring gear to the ceramic core at an elevated temperature. The resulting contraction of the gear upon cool-down, after the elastomer has been allowed to cure at the higher temperature, provides a radial compressive preload in the regenerator. The amount of preload can be adjusted by changing the bonding temperature or by modifying the configuration of the elastomer.

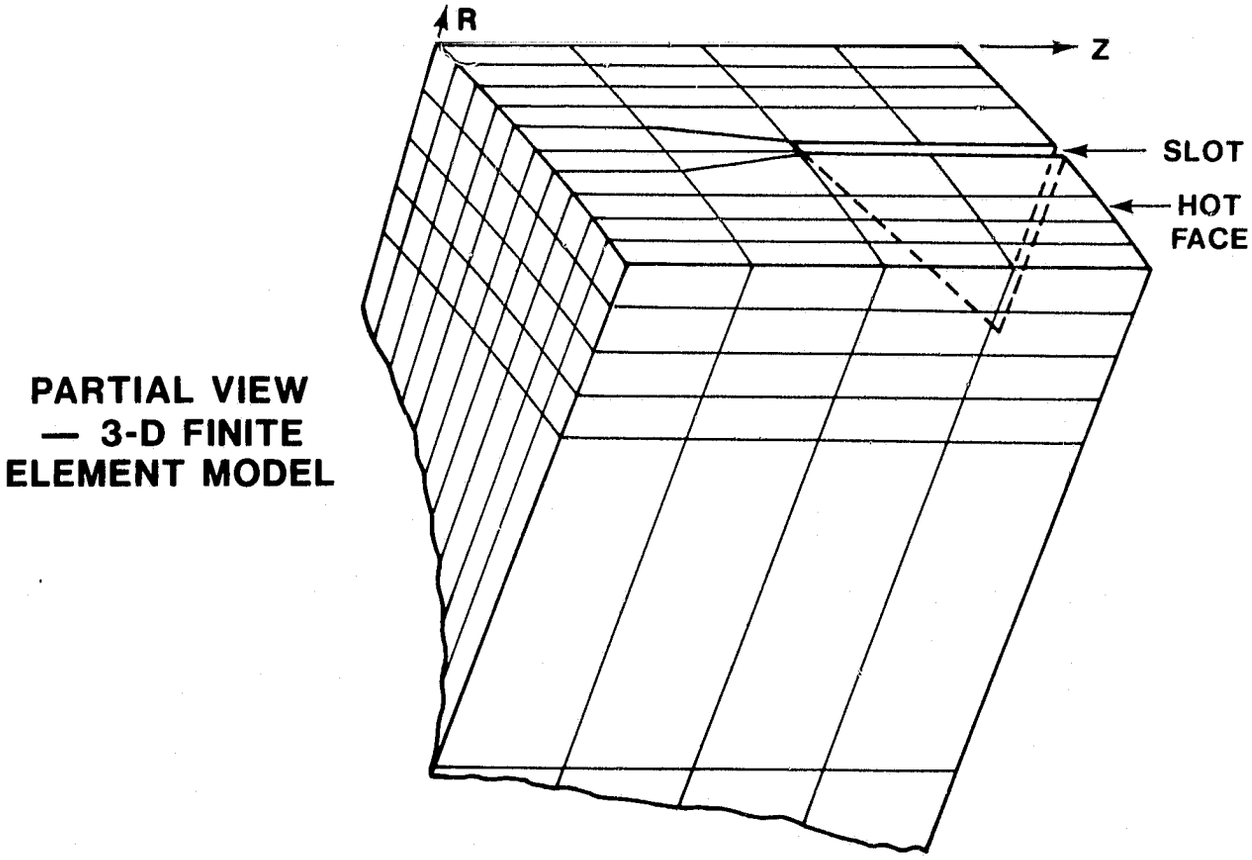

Figure 4.5 — Three Dimensional Finite Element Model

Once the matrix physical and thermal properties are established, the regenerator analytical model is applicable to the finite element method of stress analysis. This method assumes that a structure can be modeled as consisting of a number of discrete elements interconnected at a finite number of node points. The material properties of the structure being analysed, and the loads applied to the structure, determine the behavior of these elements in terms of nodal point displacement. Equilibrium equations are developed for each node point, and the solution of this set of equations determines the stress solution to the problem. Computer programs are available for both two and three-dimensional analysis.

The two-dimensional model consists of an anisentropic axisymmetric structure subjected to thermal and mechanical loads. An axisymmetric structure is any closed surface of revolution, symmetric about one axis. For a regenerator, the Z-axis should be along the axis of rotation, i.e., the axial direction; the R-axis 90° to the Z-axis and the tangential direction clockwise from the R-axis as illustrated in Figure 4.6. The elements (or element areas), which may be triangular and/or rectangular will actually be concentric circular tubes as shown.

Since variations in temperature in the tangential direction are relatively small in a regenerator this analysis is acceptable for determining approximate stress levels. In order to evaluate the effect of stress-relief slots in the rim, the three-dimensional analysis is required (Figure 4.5).

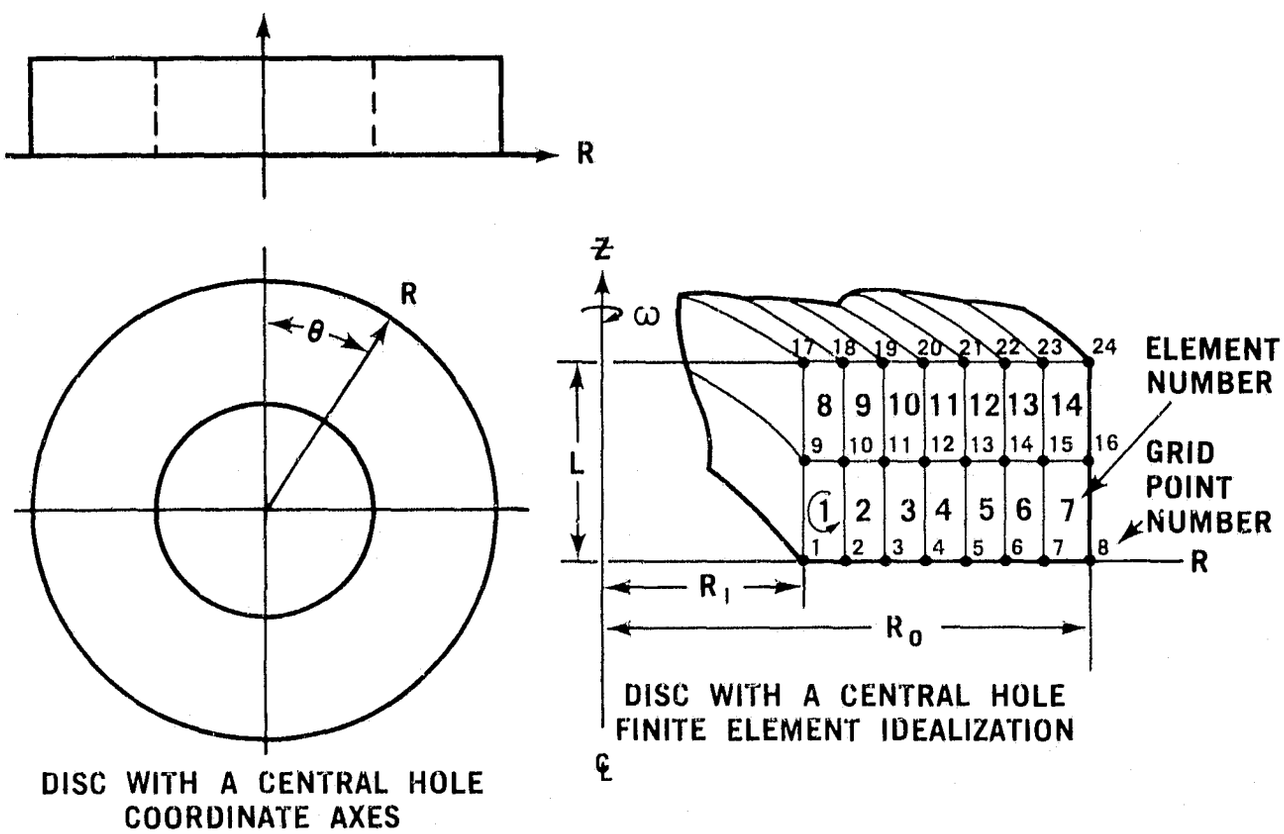

Figure 4.6 — Axisymmetric Stress Analysis Model

In the absence of available matrix property data for silicon nitride regenerators the three-dimensional stress analysis can be utilized by incorporating membrane elements. With the membrane element (Figure 4.7) solid bar properties can be utilized and the thermal stress is then determined for each side of the geometric opening. Thermal stress safety factor (S.F.) can then be approximated based on the ratio of solid bar MOR to the maximum thermal stress predicted.

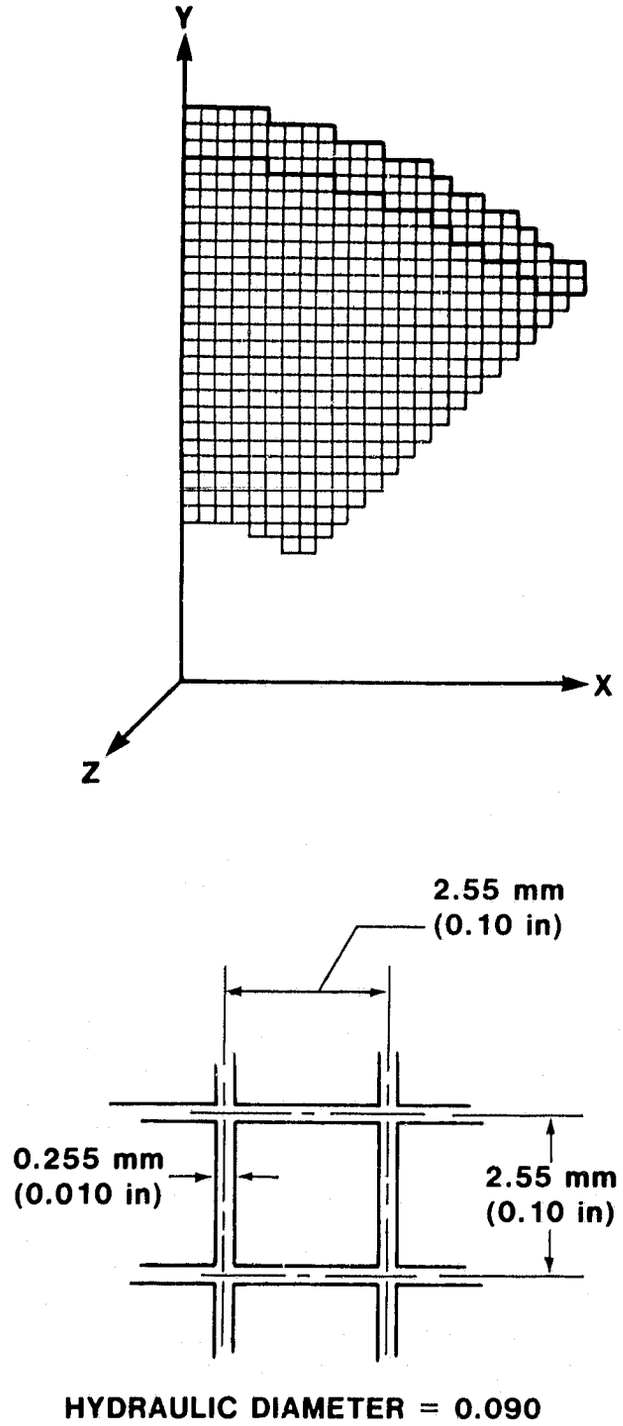

Figure 4.7 — Membrane Element Stress Analysis Model

At the present time solid bar properties have been well defined for silicon nitride at two different densities as listed on Table 4.1. These properties were incorporated into the three-dimensional analysis utilizing membrane elements. Thermal stress was then determined for each side of a square element at temperatures of 1000°C (1832°F) and 1200°C (2192°F). For economy sake, a 1/4 size finite element model was used with a 178.5 mm (7.0 in.) outside diameter and a thickness of 17.85 mm (0.7 in.). As reported previously[11], thermal stress is essentially independent of the size of the core, but is a funtion of the ratio of core outside diameter to peripheral seal inside diameter. The ratio (1.06) for this model was the same as that used for the Ford 707 regenerator core.

DENSITY (ρ) – g/cc	2.3	2.7
YOUNG'S MODULUS (M.O.E.) – KPax10^{-6}, (PSIx10^{-6})	137.8 (20)	159.8 (23.2)
SHEAR MODULUS (G) – KPax10^{-6}, (PSIx10^{-6})	55.1 (8)	68.9 (10)
POISSON'S RATIO (ν)	.25	.158
MODULUS OF RUPTURE (M.O.R.) – KPa, (PSI)	117130 (17000)	261820 (38000)
THERMAL EXPANSION (PPM) @ : °c, (°F)		
37.8 (100)	35	40
204.4 (400)	400	450
426.7 (800)	975	1100
537.8 (1000)	1325	1450
648.9 (1200)	1675	1850
815.6 (1500)	2225	2400
982.2 (1800)	2800	2975
1148.9 (2100)	3375	3550
1260 (2300)	3750	3925
STRAIN TOLERANCE (S.T. = MOR/MOE) – PPM	850	1640

Table 4.1 — Silicon Nitride Material Properties

The square passage regenerator model incorporated 954 nodes and 899 membrane elements. Nodal points on the regenerator hot face below the peripheral seal inner diameter were assigned the maximum temperature (1000°C or 1200°C). Nodal points on the regenerator cold face and on the hot face within the peripheral seal width were assigned a value of 227°C (440°F). A linear axial temperature gradient was assumed between the hot and cold faces. The thermal constraint at the rim results in tangentially oriented tensile stress components within the seal width and compressive stress below the seal inner diameter.

Figures 4.8 to 4.11 illustrate the tangential stress in the rim for the 2.7 gm/cc and 2.3 gm/cc density silicon-nitride properties at 1000°C and 1200°C. The corresponding radial stress elements are illustrated on figures 4.12 to 4.15.

The anisotropy associated with the material properties of a matrix structure is a function of the matrix cell geometry. For the square cell, the direction of maximum stiffness (or maximum apparent elastic moduli) are those perpendicular to the cell walls. The directions of minimum stiffness are along the cell diagonals. The effects of this anisotropy are evident in the results (Figures 4.8 to 4.15). The maximum stress in the square cell model is located at the point where the cell orientation is such that the maximum stiffness direction of the cell is aligned with the tangential direction of the core. Conversely, the thermal stress in the cell walls decreases as the cell minimum stiffness direction becomes aligned with the core tangential direction such that the minimum thermal stress in the core is located 45° around the periphery from the maximum stress. It should be noted that the square cell model that was utilized is typical of one fabricated by extrusion. Another method of forming a square cell regenerator is to emboss extruded ceramic tape to provide a ribbed surface and then wrap the tape around a mandrel to form a regenerator of the required diameter. A regenerator fabricated using this process would result in the maximum stiffness cell direction always tangentially oriented. Consequently, the maximum thermal stress which occurs four places, 90° apart in the extruded matrix would be continuous throughout the rim of the wrapped regenerator.

From the stress levels predicted from the membrane elements the approximate thermal stress safety factors for the two material densities at the two different regenerator inlet temperatures were determined (Table 4.2). Based on these values a silicon-nitride regenerator fabricated from a material with a density of 2.7 g/cc appears to have more than adequate thermal stress capacity. Conversely a regenerator fabricated from a material with a density of 2.3 g/cc may require one of the stress relief concepts discussed earlier.

An approximation parameter that relates mechanical properties to thermal properties of the matrix is defined as the thermal stress factor (θ), which is the ratio of strain tolerance (MOR/E) to the maximum expansion difference (Δ PPM) between the two temperature extremes of the regenerator. Since the probability of thermal failure increases with decreasing θ, it is a convenient criterion to compare and screen matrix materials on an equivalent basis.

TANGENTIAL STRESS
SILICON-NITRIDE
ρ = 2.7 gm/cc
T_{11} = 2000°F

7531	6553	4940	2876	883																		
15605	15324	14918	14416	13665	11491	7975	4378	1300														
19411	19312	19124	18786	18183	17109	15658	14123	12401	9155	4827	1397											
22034	22020	21888	21504	20746	19826	18963	18051	16926	15344	13439	11407	9050	3947	1066								
					10932	13031	14274	14535	14092	13208	11791	9676	7092	4476	1592							
									8529	10315	11042	10983	10478	9542	7972	4790	1300					
												6915	8555	9089	8709	7617	6010	3449	877			
															3463	4157	4156	3418	2279	846		
																3423	4156	4124	3608	2627	1009	
																		5568	6794	7457	7860	8000	8693
																				-861	-211	7	-24
																					-4938	-5268	-6361

Figure 4.8 — Tangential Thermal Stress for 2.7 gm/cc Density Silicon Nitride at 1093°C (2000°F)

TANGENTIAL ELEMENTS
SILICON-NITRIDE
ρ = 2.3 gm/cc
T_{11} = 2000°F

5650	4914	3700	2151	660																		
12030	11804	11472	11054	10437	8752	6069	3325	987														
15087	15000	14840	14560	14071	13224	12086	10875	9515	7007	3692	1068											
17180	17160	17045	16740	16152	15438	14754	14027	13134	11888	10395	8800	6200	3044	824								
					8502	10060	10984	11175	10832	10145	9051	7422	5437	3430	1219							
									6585	7918	8464	8419	8029	7306	6094	3657	993					
												5334	6556	6957	6670	5830	4596	2637	672			
															2667	3178	3167	2602	1735	640		
																2639	3180	3150	2753	2000	768	
																		4408	5334	5840	6142	6226	6722
																				-666	-183	-20	-53
																					-3860	-4100	-4897

Figure 4.9 — Tangential Thermal Stress for 2.3 gm/cc Density Silicon Nitride at 1093°C (2000°F)

TANGENTIAL STRESS
SILICON-NITRIDE
ρ = 2.7 gm/cc
T_{11} = 2200°F

8568	7455	5621	3272	1005																	
17754	17433	16972	16400	15547	13073	9073	4981	1479													
22085	21970	21756	21373	20685	19465	17814	16067	14108	10415	5491	1589										
25067	25050	24900	24464	23602	22556	21574	20536	19256	17457	15290	12977	9158	4491	1213							
					12438	14825	16239	16536	16033	15025	13415	11008	8068	5092	1811						
									9703	11735	12562	12495	11920	10855	9070	5449	1479				
												7867	9733	10341	9909	8665	6838	3924	997		
															3941	4730	4730	3889	2593	963	
																3895	4730	4693	4106	2989	1148
																		6260	7656	8410	8870	9024	9816
																				-972	-230	17	-18
																					-5536	-5911	-7154

Figure 4.10 — Tangential Thermal Stress for 2.7 gm/cc Density Silicon Nitride at 1204°C (2200°F)

TANGENTIAL ELEMENTS
SILICON-NITRIDE
ρ = 2.3 gm/cc
T_{11} = 2200°F

6480	5636	4244	2467	756																	
13800	13538	13157	12678	11970	10037	6960	3818	1132													
17303	17204	17019	16700	16138	15166	13861	12473	10913	8036	4234	1225										
19703	19700	19548	19200	18525	17705	16921	16087	15063	13635	11920	10090	7110	3491	945							
					9750	11539	12600	12817	12423	11635	10380	8512	6235	3933	1398						
									7552	9081	9707	9655	9208	8379	6989	4194	1139				
												6117	7519	7979	7649	6687	5271	3025	771		
															3059	3645	3632	2983	1989	739	
																3026	3646	3612	3157	2296	880
																		4993	6055	6635	6982	7079	7647
																				-763	-210	-30	-60
																					-4368	-4645	-5559

Figure 4.11 — Tangential Thermal Stress for 2.3 gm/cc Density Silicon Nitride at 1204°C (2200°F)

RADIAL STRESS
SILICON-NITRIDE

ρ = 2.7 gm/cc

T

												1943	1063	320
												1950	1090	339
												1685	939	296
												1010	511	155
												·355	·477	·226
											778	·450	·1428	·863
											821	435	119	
											·113	·107	·38	
											·1704	·1260	·479	
										·1263	·2161	·2553	·1300	
										·1014	·768	·263		
										·2563	·1800	·635		
									·2242	·2925	·2973	·1397		
									·1961	·1356	·473			
									·3619	·2276	·748			
								·4389	·4015	·2899	·1066			
							·3675	·3983	·3580	·1592				
							·3699	·2542	·889					
						·3596	·3644	·3070	·1300					
						·3764	·2422	·819						
					·3989	·3367	·2371	·876						
				·3343	·2911	·2139	·846							
				·4390	·2880	·1009								
				[illegible]	·706									
				·7624	·8822									

Figure 4.12 — Radial Thermal Stress for 2.7 gm/cc Density Silicon Nitride at 1093°C (2000°F)

RADIAL ELEMENTS
SILICON-NITRIDE

ρ = 2.3 gm/cc
T_{11} = 2000° F

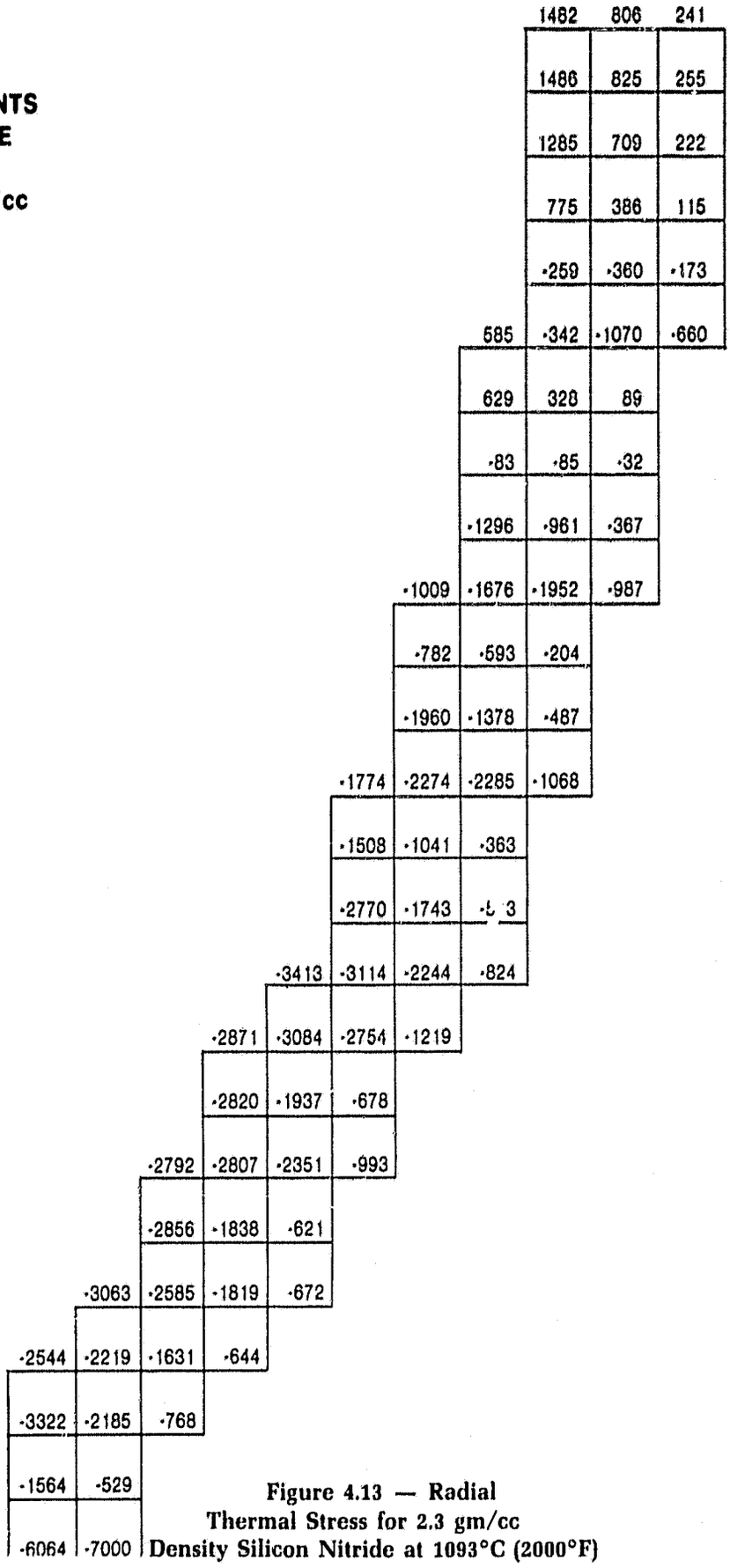

Figure 4.13 — Radial Thermal Stress for 2.3 gm/cc Density Silicon Nitride at 1093°C (2000°F)

RADIAL STRESS
SILICON-NITRIDE
ρ = 2.7 gm/cc
T_{11} = 2200°F

| | | |

RADIAL ELEMENTS
SILICON-NITRIDE
ρ = 2.3 gm/cc
T_{11} = 2200°F

									1700	925	276
									1705	945	292
									1474	814	254
									888	442	131
									-297	-413	-198
								671	-392	-1226	-756
								721	377	102	
								-95	-97	-36	
								-1486	-1102	-420	
							-1156	-1922	-2239	-1132	
							-896	-680	-234		
							-2249	-1580	-559		
						-2034	-2608	-2621	-1225		
						-1730	-1194	-416			
						-3177	-2000	-657			
					-3914	-3571	-2573	-945			
				-3293	-3537	-3158	-1400				
				-3234	-2221	-777					
			-3200	-3219	-2700	-1139					
			-3276	-2108	-712						
		-3513	-2965	2086	-771						
	-2918	-2545	-1870	-739							
	-3810	-2505	-880								
	-1794	-606									
	-6890	-7940									

Figure 4.15 — Radial Thermal Stress for 2.3 gm/cc Density Silicon Nitride at 1204°C (2200°F)

DENSITY (ρ) — g/cc	2.3		2.7	
TEMPERATURE, °C, (°F)				
H.P. INLET	227 (440)		227 (440)	
L.P. INLET	1093 (2000)	1204 (2200)	1093 (2000)	1204 (2200)
M.O.E., KPa x 10^{-6}, (PSI x 10^{-6})	137.8 (20)		159.8 (23.2)	
M.O.R., KPa, (PSI)	117130 (17000)		261820 (38000)	
MAXIMUM THERMAL STRESS (σT_{MAX}), KPa, (PSI)	118370(17180)	135733(19700)	151814(22034)	172711 (25067)
THERMAL STRESS SAFETY FACTOR (S.F.)	.99	.86	1.72	1.52
THERMAL STRAIN DIFFERENCE (ΔPPM)	2725	3105	2845	3220
S.T. (PPM)	850		1640	
THERMAL STRESS FACTOR (θ)	.31	.27	.58	.51

Table 4.2 — Silicon Nitride Regenerator Thermal Stress

Based on the solid bar properties of the silicon nitride materials utilized for the thermal stress analysis, the thermal stress factors (θ) are listed on Table 4.2 for these materials. This approximation parameter (θ) can be utilized as a baseline for evaluating matrix structures that are fabricated with these or other variations of silicon nitride materials.

From the results in Table 4.2, it would appear that a silicon nitride matrix material with a minimum value of θ equal to .32 could be feasible for a regenerator application with inlet temperatures up to 1204°C (2200°F). Matrix materials with θ less than .32 might require the incorporation of stress relief techniques.

In summary, the feasibility of silicon nitride with respect to thermal stress capacity appears to be promising. The analysis presented provides a guideline for the matrix material requirements based on the thermal stress factors (θ) of the solid bar materials evaluated.

5.0 AEROTHERMODYNAMIC PERFORMANCE

5.1 PERFORMANCE PARAMETERS

The purpose of a rotary regenerator is to transfer heat energy effectively from one working fluid to another by storing heat energy in the matrix with minimal conductance loss while minimizing fluid pressure drop across the matrix. The essential parameters required for accurate regenerator performance and sizing prediction are the basic heat transfer (J = Stanton-Prandtl No. = Colburn No.) and pressure drop (F = Fanning Friction Factor) characteristics for the matrix surface geometries being considered. To obtain the heat transfer and pressure drop characteristics for the matrices evaluated, a transient shuttle rig technique is utilized.

In the design of a regenerator for a specific engine application, a compromise is usually required between the final package size and matrix surface geometry selected to obtain specified performance benchmarks. Consequently, the designer must be able to evaluate the effect a change in package size and/or fin geometry will have on regenerator effectiveness and pressure drop. Regenerator pressure drop ($\Delta P/P$) and overall number of heat transfer units (U_O) can be expressed in terms of flow conditions, package size, and matrix fin parameters [12] as follows:

$$\frac{\Delta P}{P} = \underbrace{\left[\frac{2W\mu RT}{gP^2}\right]}_{\text{(FLOW CONDITIONS)}} \underbrace{\left[\frac{L}{A_F}\right]}_{\text{(PACKAGE SIZE)}} \underbrace{\left[\frac{C_1}{\sigma DH^2}\right]}_{\text{(FIN PARAMETERS)}}$$

$$U_O = \underbrace{\left[\frac{2\mu}{WNPR^{2/3}}\right]}_{\text{(FLOW CONDITIONS)}} \underbrace{\left[L \cdot A_F\right]}_{\text{(PACKAGE SIZE)}} \underbrace{\left[\frac{C_2\sigma}{DH^2}\right]}_{\text{(FIN PARAMETERS)}}$$

For a balanced regenerator the theoretical effectiveness (E_T) can then be approximated as follows:

$$E_T \approx \frac{U_O}{U_O + 1} \qquad (\text{IF:} x^* = 1)$$

Where:

X_2	=	Reynold's No. exponent for Colburn No. ($J = C_2\ RE^{X_2}$)
C_1	=	Fanning Friction Factor Constant for Laminar Flow ($F = C_1/RE$)
C_2	=	Colburn No. Constant for Laminar Flow
σ	=	Open Area Ratio
DH	=	Hydraulic Diameter
W	=	Air Flow Rate
μ	=	Viscosity
R	=	Universal Gas Constant

μ = Viscosity

R = Universal Gas Constant

T = Average Temperature

g_c = Proportionality Factor in Newton's Second Law

L = Flow Length

A_F = Frontal Area of the Regenerator

ΔP = Pressure Drop

P = Inlet Pressure

E_T = Theoretical Effectiveness = ϕ (U_O, X^*)

X^* = Flow Capacity Rate Ratio = C_{MIN}/C_{MAX}

U_O = Number of Heat Transfer Units (NTU)

PR = Prandtl Number

C_{MIN} = Minimum Flow Capacity Rate

C_{MAX} = Maximum Flow Capacity Rate

Utilizing the above relationships, the parametric curves shown on Figure 5.1.1 were constructed to evaluate the effect of package size and fin parameters on regenerator performance for a fixed set of flow conditions. Closer examination of these parametric curves reveals four distinct zones of interest (Figure 5.1.2). Alterations in package size and/or fin parameters which move the baseline point into zone 3 are highly desirable, since effectiveness increases while pressure drop decreases. Conversely, movement into zone 1 is detrimental, since effectiveness decreases while pressure drop increases. Zones 2 and 4 are compromise regions where both effectiveness and pressure drop increase or decrease respectively.

In addition to regenerator package size and matrix surface geometry, the thermal conductivity of the matrix material must also be considered. The effect of thermal conductivity on regenerator heat transfer effectiveness can be illustrated by the following expressions:

E_T = Theoretical Effectiveness = ϕ (U_O, X^*)

E_R = Correction Factor Due to Rotation

λ = Conduction Parameter = $\dfrac{K_M A_F (1-\sigma)}{C_{MIN} L}$

η_C = Thermal Conductivity Correction Factor = $\dfrac{1}{1 + \lambda}$

E_A = Actual Effectiveness = $\eta_C E_R E_T$

Where:

K_M = Thermal Conductivity of the Material in the Axial Direction

In order to evaluate the influence of thermal conductivity, the parametric curves shown in Figure 5.1.3 were generated. The procedures for utilization of the parametric curves of Figures 5.1.1 and 5.1.3 are described in the appendix. Once the matrix geometry is selected and the regenerator package size and shape is determined, the conduction parameter (λ) must be minimized to attain maximum thermal efficiency (E_A).

5.2 INFLUENCE OF SILICON NITRIDE ON REGENERATOR PACKAGE SIZE

For the present generation of oxide ceramic materials, such as MAS and AS, conduction losses are minimal regardless of regenerator shape due to their extremely low values of thermal conductivity (K_M). In the event oxide ceramic materials are not suitable for 1200°C (2192°F), thermal conduction loss becomes more prominent when materials such as silicon nitride are considered. While this material has higher temperature capability, it also possesses much higher thermal conductivity (K_M). For example, the K_M of the oxide ceramics are less than .004 CAL./CM.–SEC.–°F (1.0 BTU/HR.–FT. –°F), whereas the K_M of silicon nitride can vary from .017 to .051 CAL./CM.–SEC.–°F (4.0 to 12.0 BTU/HR.–FT.–°F), depending on the density and application temperature of the material. This factor is especially critical near engine idle conditions where maximum thermal efficiency is desired for maximum fuel economy at part power. At this condition the flow capacity rate (C_{MIN}) through the regenerator is at its minimum value, which in turn maximizes the conduction parameter (λ).

Due to the thermal conductivity characteristics of silicon nitride, alterations in present day design philosophy appear to be required. A primary objective for current vehicular gas turbine engines is the design of a compact, efficient heat exchanger in order to attain lighter weight and lower cost. Utilization of matrix geometries with small hydraulic diameters (DH) and high surface area to volume ratios (β) are essential for attaining this objective. While the overall number of heat transfer units (U_O) is proportional to volume (A_FL), pressure drop is dependent on the ratio of thickness (L) to frontal (A_F) of the regenerator. Consequently, current regenerators possess a low thickness to outside diameter ratio (L/A_F) in order to minimize pressure loss for a fixed value of effectiveness (E_T).

When thermal conductivity effects are significant, the value of U_O must be increased and/or the value of λ must be minimized in order to attain the desired thermal efficiency (E_A). In effect any increase in U_O results in an increase in the volume requirement for the regenerator. Conversely a reduction in λ can be accomplished by reshaping a given heat exchanger volume, by increasing the thickness to outside diameter ratio. Unfortunately, this technique would also increase the pressure drop through the matrix. An alternate approach is the selection of a matrix geometry with a greater hydraulic diameter.

In order to illustrate the effect of thermal conductivity on regenerator design the following example has been selected. A typical future 100 hp passenger car gas turbine engine was selected to establish the flow conditions and performance design requirements for the regenerator (Table 5.2.1).

For discussion purposes two fin configurations were selected from the existing matrix sample size (Table IV.B.1 and IV.B.2 in Reference 13). Matrix 19 represents the most efficient compact fin based on the present day design philosophy to produce the smallest heat exchanger volume to attain the desired performance level. In order to illustrate the influence of hydraulic diameter, matrix 3 was selected, which has a 67% larger hydraulic diameter compared to matrix 19. The pertinent fin parameters for these matrix geometries are listed on Table 5.2.2.

While matrix 19 represents existing tooling that is capable of producing this configuration with the desirable minimum material thickness of .061 mm (.0024 in.), matrix 3 was fabricated from tooling that was produced 5 years ago. With present day technology matrix 3 could be fabricated with a significant reduction in material thickness. Consequently, the pertinent fin parameters from matrix 3 were redefined (Table 5.2.2) based on a material thickness of .127 mm (.0050 in.) instead of .216 mm (.0085 in.). The basic performance characteristics (F and J) are based on the actual geometric opening of the fin configuration with the material wall thickness factored out. To maintain the same heat transfer (J) and pressure drop (F) characteristics for the matrix 3 geometry with reduced material thickness, the geometric opening is kept constant to maintain the same hydraulic diameter (DH) by adjusting the cell density (N) proportionately to the material thickness change (Table 5.2.2).

Utilizing matrix 19, a singular regenerator that is 36.8 CM. O.D. X 5.1 CM. I.D. X 7.1 CM. thick (14.5 in. x 2.0 in. x 2.80 in.) will yield the desired effectiveness (E_A = 97.2%) and pressure drop (Δ P/P = 2.40%) at idle flow conditions (N_G = 50%) when fabricated with the current oxide ceramics (K_M = .0026 CAL./CM.–SEC.–°C). The regenerator size requirement when fabricated with the modified matrix 3 geometry to produce the identical performance level can be determined from the parametric curves of Figure 5.1.1.

For illustration purposes the matrix 19 regenerator will be selected as the initial reference regenerator (Case 1, Table 5.2.3). Utilizing the parametric curves for performance (Figure 5.1.1) and conduction (Figure 5.1.3) the size required for the modified matrix 3 (3M) regenerator was determined (Case 2, Table 5.2.3) for equivalent performance. If fabricated with the current oxide ceramics, the matrix 3M regenerator would not be acceptable since the volume required is 2.42 times greater than the matrix 19 regenerator.

A second comparison can be made for these regenerators by assuming they are fabricated from silicon-nitride material with a mean value for thermal conductivity of .034 CAL/CM–SEC.–°F (8 BTU/HR.–FT.–°F). Cases 3 and 4 represent the performance at part power (N_G = 50%) for the matrix 19 and 3M regenerators, respectively. In this instance the high volume matrix 3M regenerator results in a 2.1% gain in effectiveness compared to the matrix 19 regenerator. For this engine configuration the matrix 3M regenerator would increase fuel economy approximately 13% at this condition.

In order to compare these matrices on an equal volume basis the frontal area (A_F) and thickness (L) of the matrix 19 regenerator can be increased proportionately

to maintain a constant pressure drop until the volume is equivalent to the matrix 3M regenerator (Case 5). In spite of the volume and pressure drop equivalence, the matrix 19 regenerator would still be .8% lower on actual effectiveness (E_A), which would increase engine SFC approximately 5%, even though theoretical effectiveness (E_T) was increased substantially (1.4%).

An additional option would be to reshape the enlarged matrix 19 regenerator in order to reduce the loss due to conduction without reducing the volume, which in effect maintains the desirable value for theoretical effectiveness (E_T). Case 6 illustrates the effect of increasing the length to frontal area ratio (L/A_F) for the enlarged matrix 19 regenerator. A 32% increase in L/A_F reduced the conduction loss enough to attain effectiveness (E_A) equivalence with the matrix 3M regenerator (Case 4). Unfortunately the pressure drop for the matrix 19 regenerator increased an additional .80%. This would result in a 2.25% penalty on fuel economy in addition to a loss in horsepower.

In summation, regenerators fabricated with the current oxide ceramics, which have low thermal conductivities, require compact fin geometries to attain minimum volume for the desired thermal efficiency. In order to minimize pressure loss, the length to frontal area ratios must also be minimized.

For fabrication of high temperature regenerators requiring materials with high thermal conductivity, such as silicon-nitride, a substantial increase in heat exchanger volume is required to recover the loss in thermal efficiency due to thermal conductivity. This factor can add additional complexities to engine packaging problems.

In order to minimize conduction losses it is desirable to package the regenerator with a higher length to frontal area ratio by incorporating less compact fin geometries (larger hydraulic diameters) to maintain the desired level of pressure drop.

REGENERATOR PERFORMANCE VS. FIN PARAMETERS & CORE SIZE AT CONSTANT FLOW CONDITIONS

$U_0 = \frac{2\mu}{W N_{PR}^{2/3}} A_F L \frac{C_2 \sigma}{DH^2}$ $\quad E = \frac{U_0}{U_0 + 1}$ (IF : X' = 1) $\quad$ ⊗ DESIGN OR BASELINE PT.

$\frac{\Delta P}{P} = \frac{2\mu WRT}{g_c P^2} \frac{L}{A_F} \frac{C_1}{\sigma DH^2}$ $\quad F = C_1 N_{RE}^{X_1}$, $J = C_2 N_{RE}^{X_2}$ $(X_1 = X_2 = -1)$

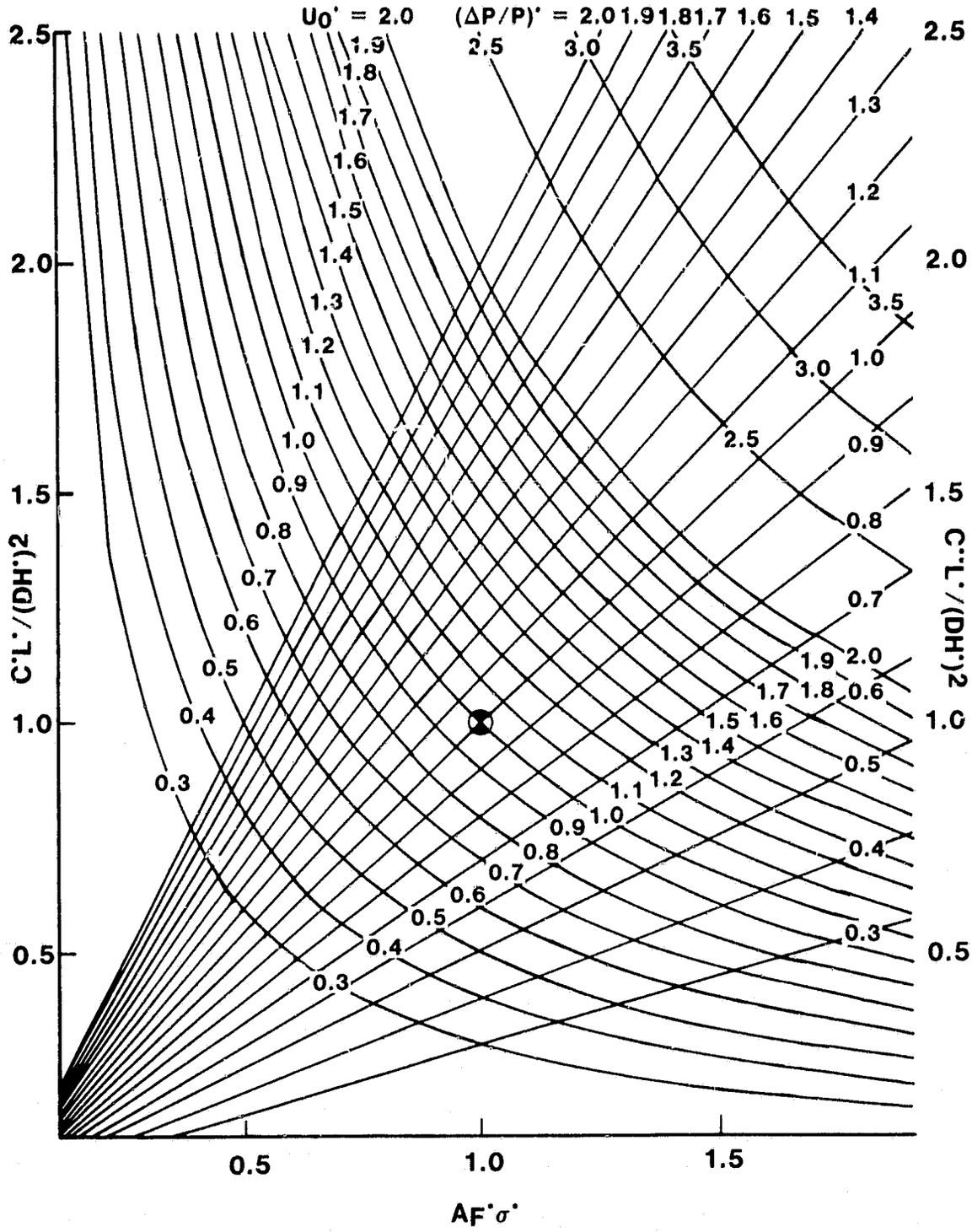

Figure 5.1.1 — Regenerator Performance with Respect to Package Size and Fin Parameters for Constant Flow Conditions

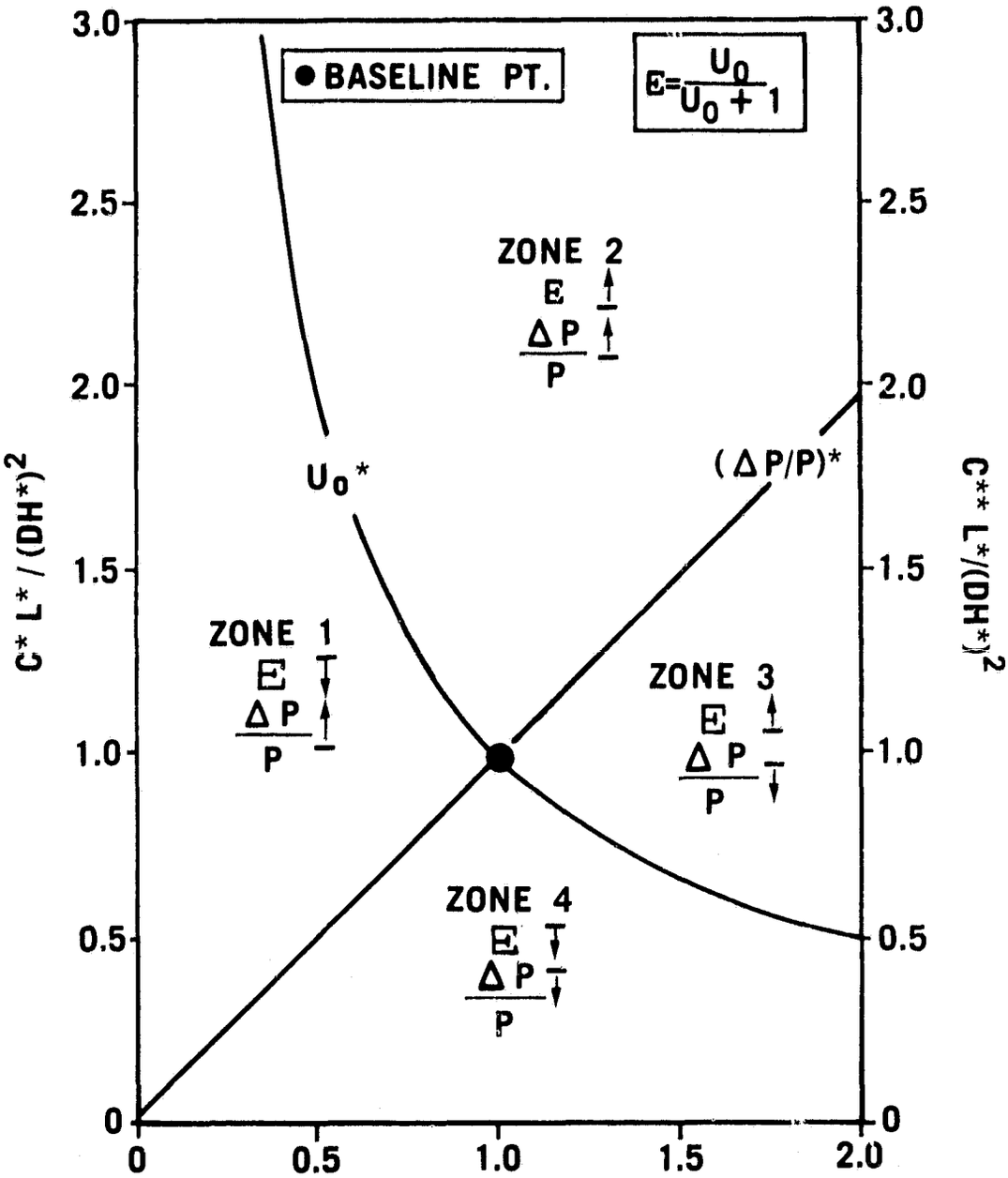

Figure 5.1.2 — Regenerator Performance Zones

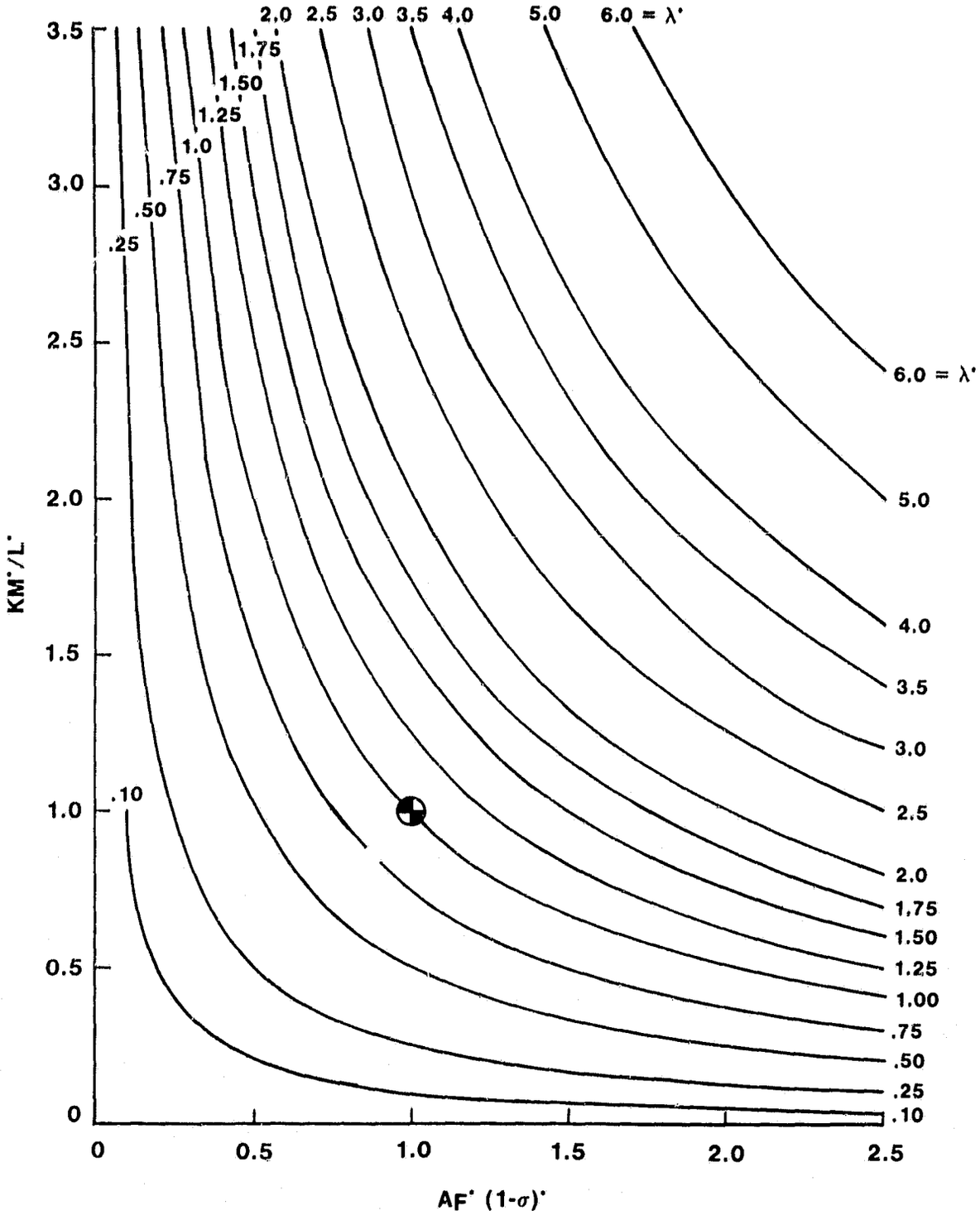

Figure 5.1.3 — Thermal Conductivity with Respect to Package Size and Fin Parameters for Constant Flow Conditions

N_{GG} %	FLOW CONDITIONS	REGENERATOR SIDE	
		HIGH PRESSURE	LOW PRESSURE
100	FLUID MASS FLOW RATE, Kg./SEC., (LB./SEC.)	.374 (.821)	.382 (.840)
	INLET TEMPERATURE, °C, (°F)	244 (471)	943 (1730)
	INLET PRESSURE, KPa, (PSIA)	493.6 (71.64)	111.9 (16.24)
	DESIGN PRESSURE DROP, %	.25	6.06
	DESIGN EFFECTIVENESS, %	90.5	
50	FLUID MASS FLOW RATE, Kg./SEC., (LB./SEC.)	.104 (.228)	.105 (.231)
	INLET TEMPERATURE, °C, (°F)	88 (191)	1093 (2000)
	INLET PRESSURE, KPa, (PISA)	165.8 (24.06)	103.8 (15.06)
	DESIGN PRESSURE DROP, %	.63	1.78
	DESIGN EFFECTIVENESS, %	97.4	

Table 5.2.1 — Regenerator Flow Conditions

CODE:

R — RECTANGULAR

I.T. — ISOSCELES TRIANGULAR

S.T. —SINUSOIDAL TRIANGULAR

H — HEXAGONAL

$$F = C_1 RE^{X_1}$$

$$J = C_2 RE^{X_2}$$

$$\frac{\Delta P.P}{L} = \frac{WT^{1.673}}{AF} \qquad \frac{NTU}{L} = A\left[\frac{AFT^{0.673}}{W}\right] - X_2$$

MATRIX NO.	TYPE OF FIN	X FINS/CM (FINS/IN.)	Y ROWS/CM (ROWS/IN.)	N HOLES/CM^2 (HOLES/IN.^{2})	S MM (IN.)	B MM (IN.)	H MM (IN.)	PH MM (IN.)	AR PH/H	σ	DH MM (IN.)	β M^2/M^3 (FT.^{2}/FT.^{3})	C X10^5	A X10^2	C_1	X_1	C_2	X_2	J F @ RE=100
19	S.T.	15 (38)	13.6 (34.5)	203.9 (1311)	.061 (.0024)	.061 (.0024)	.676 (.0266)	1.336 (.0526)	1.98	.787	.579 (.0228)	5422 (1653)	1.38	6.50	16.1	− 1	3.94	− 1	.245
3	R	8.3 (21)	8.7 (22)	71.6 (462)	.216 (.0085)	.216 (.0085)	.940 (.037)	1.211 (.0477)	1.29	.669	.968 (.0381)	2765 (843)	.54	2.10	14.9	− 1	4.18	− 1	.281
3M	R	8.9 (22.6)	9.4 (23.8)	84 (538)	.127 (.005)	.127 (.005)	.940 (.037)	1.123 (.0442)	1.19	.780	.968 (.0381)	3224 (983)			14.9	− 1	4.18	− 1	.281

Table 5.2.2 — Regenerator Matrix Fin Parameters

CASE NO.	REF. CASE NO.	MATRIX NO.	B=S IN.	σ	DH IN.	C_1	C_2	D_0 IN.	A_F FT.^{2}	L IN.	VOL IN.^{3}	$A_F{}^*\sigma$	$\frac{C^*L^*}{(DH^*)^2}$	$\frac{C^{**}L^*}{(DH^*)^2}$	$(\Delta P\ P)^*$	$U_0{}^*$	U_0	E_T %	$(\Delta P\ P)_T$ %	K_M BTU / HR.*FT.-F	$\frac{K_M{}^*}{L^*}$	$\frac{A_F{}^*}{(1-\sigma)^*}$	λ^*	λ	η_c	E_A %	$\frac{L}{A_F}$	VOL*
1		19	.0024	.787	.0228	16.1	3.94	14.5	1.125	2.80	454	1.0	1.0	1.0	1.0	1.0	39.0	97.5	2.40	.60	1.0	1.0	1.0	.00284	.997	97.2	.207	1.0
2	1	2M	.005	.780	.0381	14.9	4.18	13.8	1.017	7.50	1098	.90	.89	1.02	1.0	.923	36.0	97.3	2.40	.60	.373	.934	.35	.001	.999	97.2	.615	2.42
3	1	19	.0024	.787	.0228	16.1	3.94	14.5	1.125	2.80	454	1.0	1.0	1.0	1.0	1.0	39.0	97.5	2.40	8.0	13.3	1.0	13.3	.0379	.963	93.9	.207	1.0
4	2	2M	.005	.780	.0381	14.9	4.18	13.8	1.017	7.50	1098	1.0	1.0	1.0	1.0	1.0	36.0	97.3	2.40	8.0	13.3	1.0	13.3	.0133	.987	96.0	.615	2.42
5	3	19	.0024	.787	.0228	16.1	3.94	18.0	1.75	4.36	1098	1.55	1.55	1.55	1.0	2.42	94.4	98.9	2.40	8.0	.64	1.56	1.0	.0379	.963	95.2	.207	2.42
6	5	19	.0024	.787	.0028	16.1	3.94	16.8	1.525	5.0	1098	.87	1.15	1.15	1.35	1.0	94.4	98.9	3.19	8.0	.87	.87	.75	.0284	.972	96.1	.273	2.42

Table 5.2.3 — Regenerator Aerothermodynamic Performance

REFERENCES

1. Cook, J. A., Fucinari, C. A., Lingscheit, J. N., Rahnke, C. J., Rao, V. D. N., Quarterly Progress Report for Oct.-Dec. 1977, No. NASA CR-135380, Ceramic Regenerator Systems Development Program, NASA Contract No. DEN3-8, Feb. 1978.

2. Conceptual Design Study of Improved Automotive Gas Turbine Powertrain — Final Report, No. NASA CR-159580, NASA Contract No. DEN3-37, May 1979.

3. McLean, A. F., Baker, R. R., Brittle Materials Design — High Temperature Gas Turbine, AMMRC-CTR-76-31, Oct. 1976.

4. Grathwohl, G., Porz, H., Thümmler, F., Oxide Phases in Reaction Bonded Silicon Nitride and Their Relevance of High Temperature Mechanical Properties, Proceedings of British Ceramic Society, July, 1978, pp. 129-140.

5. Baumgartner, H. R., Washburn, M. E., High Temperature Properties of Reaction Bonded Silicon Nitride, Proceedings of Army Materials Technology Conference, Nov. 1973, pp. 479-491.

6. Singhal, S. C., Oxidation and Corrosion — Erosion of Si_3N_4 and SiC, ibid., pp. 533-549.

7. Probst, H. B., Sanders, W. A., High Gas Velocity Burner Tests on Silicon Carbide and Silicon Nitride at 1200°C, ibid., pp. 493-531.

8. Brooks, S., Meadowcraft, D. B., The Corrosion of Silicon Based Ceramics in a Residual Fuel Oil Fired Environment, Proceedings of the British Ceramic Society, July 1978, pp. 129-140.

9. Mayer, M. I., Riley, I. L., Sodium Ion Assisted Oxidation of Reaction Bonded Silicon Nitride, ibid., pp. 251-264.

10. Cook, J. A., Fuginari, C. A., Lingscheit, J. N., and Rahnke, C. J., Final Annual Report for Period July 1975 to Sept. 1976, Automotive Gas Turbine Ceramic Regenerator Design and Reliability Program, No. COO-2630-18, ERDA Contract No. E(11-1) 2630, Oct. 1976.

11. Cook, J. A., Fucinari, C. A., Lingscheit, J. N., Rahnke, C. J., Vallance, J. K., Quarterly Progress Report for April-June 1978, No. NASA CR-159432, Ceramic Regenerator Systems Development Program, NASA Contract No. DEN3-8, Sept. 1978.

12. Fucinari, C. A., "The Effect of Fin Geometry and Manufacturing Process on Ceramic Regenerator Thermodynamic Performance, Journal of Engineering for Power, Trans. ASME, Series A, Vol. 99, Oct. 1977, pp. 638-644.

13. Fucinari, C. A., Lingscheit, J. N., Vallance, J. K., Progress Report for July-Dec. 1978, No. NASA CR-159541, Ceramic Regenerator Systems Development Program, NASA Contract No. DEN 3-8, March 1979.

APPENDIX

In order to utilize the parametric performance curves (Figure 5.1.1), the effectiveness and pressure drop must be determined for the reference or baseline regenerator size and fin geometry at a given set of flow conditions. Once the reference regenerator size and fin geometry have been selected, the following expressions must be determined for each change in fin geometry or package size:

C^*	=	Ratio of Fanning Friction Factor constant with respect to reference laminar flow Fanning Friction Factor constant, C_1/C_{1B}
C^{**}	=	Ratio of Colburn No. constant with respect to reference laminar flow Colburn No. constant, C_2/C_{2B}
L^*	=	Flow length or thickness ratio with respect to reference regenerator thickness, L/L_B
DH^*	=	Hydraulic diameter ratio with respect to reference fin hydraulic diameter, DH/DH_B
A_F^*	=	Frontal area ratio with respect to reference regenerator frontal area, A_F/A_{F_B}
σ^*	=	Ratio of open area percentage with respect to reference fin open area ratio, σ/σ_B
U_o^*	=	Number of heat transfer units ratio with respect to reference regenerator number, U_o/U_{oB}
$(\Delta P/P)^*$	=	Pressure drop ratio with respect to reference regenerator pressure drop, $(\Delta P/P)/(\Delta P/P)_B$

After the above ratios are determined, the effect of alterations in fin geometry and/or package size can be estimated with respect to the reference or baseline configuration performance, provided the regenerator flow conditions are not altered.

In order to utilize the parametric thermal conductivity curves (Figure 5.1.3), the conduction parameter must be determined for the reference or baseline regenerator size, fin geometry and material at a given set of flow conditions. Once the reference regenerator size, fin geometry and material have been selected, the following expressions must be determined:

K_M^*	=	Ratio of material thermal conductivity with respect to the reference material conductivity, K_M/K_{M_B}
L^*	=	Flow length or thickness ratio with respect to reference regenerator thickness, L/L_B
A_F^*	=	Frontal area ratio with respect to reference regenerator frontal area, A_F/A_{F_B}
$(1-\sigma)^*$	=	Ratio of solid cross-sectional area to reference solid cross-sectional area percentage, $(1-\sigma)/(1-\sigma_B)$
λ^*	=	Ratio of conduction parameter to reference conduction parameter, λ/λ_B

After these ratios are determined, the effect of alterations in fin geometry, material and package size can be estimated with respect to the reference conduction condition, provided the flow conditions remain constant.

1. Report No	2. Government Accession No.	3. Recipient's Catalog No.
NASA CR-159713		

4. Title and Subtitle	5. Report Date
Feasibility Study of Silicon Nitride Regenerators	Oct. 1979
	6. Performing Organization Code
7. Author(s)	8. Performing Organization Report No
C. A. Fucinari and V. D. N. Rao	
	10. Work Unit No.
9. Performing Organization Name and Address Research Staff Ford Motor Co. Dearborn, Michigan 48121	11. Contract or Grant No. Den 3-8
12. Sponsoring Agency Name and Address Department of Energy Automotive Technology Division Washington, D.C. 20545	13. Type of Report and Period Covered Contractor Report
	14. Sponsoring Agency Report No. DOE/NASA/0008-79/10

15. Supplementary Notes Interim Report Prepared under Interagency Agreement EC-77-A-31-1040

Project Manager, Thomas J. Miller, Transportation Propulsion Division, and Dr. Thomas P. Herbell, Materials and Structures Division, NASA Lewis Research Center, Cleveland, Ohio 44135

16. Abstract

This report examines the feasibility of silicon nitride as a regenerator matrix material for applications requiring inlet temperatures above 1000°C (1832°F). Using the present generation oxide ceramics as a reference, silicon nitride was examined from a material characteristics, manufacturing, thermal stress and aerothermodynamic viewpoint.

17. Key Words (Suggested by Author(s))	18. Distribution Statement
Heat Exchangers Ceramic Regenerator Systems Ceramic Materials Heat Exchanger Manufacturing	Unclassified — unlimited STAR Category 85 DOE Category UC-96

19. Security Classif. (of this report)	20. Security Classif. (of this page)	21. No. of Pages	22. Price*
Unclassified	Unclassified	52	

*For sale by the National Technical Information Service, Springfield, Virginia 22161

NASA-C-168 (Rev. 10-75)